Communications on Applied Nonlinear Analysis
ISSN: 1074-133X
Vol 33 No. 1s (2026)

Stability Analysis and Optimal Control of Zika Virus Transmission Using the Q − Homotopy Analysis Transform Method

J. Sujatha[1], N. Magesh [2], C. Murugesan [3 *], G. Tamilpreethi [4]

[1,2,3 *] Post-Graduate and Research Department of Mathematics

Government Arts College for Men, Krishnagiri 635001, Tamilnadu, India.

[4] Department of Mathematics

Government College of Engineering, Bargur-635104, Tamilnadu, India.

e-mail: [1] sujiselva8815@gmail.com, https://orcid.org/0009-0006-2521-7304,

[2] nmagi 2000@yahoo.co.in, https://orcid.org/0000-0002-0764-8390,

[3 *] cmurugesan27@gmail.com, https://orcid.org/0009-0000-4233-8825,

[4] tamilpreethig@gmail.com, https://orcid.org/0000-0003-3453-0029.

Article History:

Received: 03-02-2026

Revised: 30-03-2026

Accepted: 10-04-2026

Abstract:

The Zika virus (ZIKV) poses significant public health challenges due to its rapid transmission and severe effects on pregnant women and new-borns. In this paper, we develop a compartment mathematical model to study the transmission dynamics of the Zika virus between human and mosquito populations. The human population is divided into susceptible, exposed, infected, pregnant, infected infant, and recovered classes, while the mosquito population includes susceptible, exposed, and infected compartments. The basic reproduction number R_0 is derived using the next generation matrix method to determine the threshold condition for disease persistence. By examining the existence and uniqueness, local and global stability analyses of both the disease free and endemic equilibrium are performed using linearization and Lyapunov function techniques. We incorporated optimal control to identify effective prevention, treatment, and vector management strategies in the model. To obtain approximate analytical solutions, we employ the q − homotopy analysis transform method (q − HATM), which provides a rapidly convergent series solution without restrictive assumptions. The results demonstrate that reducing the contact rate and enhancing recovery significantly decrease R_0 and prevent disease outbreak.

Keywords and Phrases : Stability Analysis, Zika virus model, Epidemic Model, Non-linear differential equations, Mathematical Models, Existence and uniqueness, Optimal control, q − Homotopy Analysis Transform Method.

2020 Mathematics Subject Classification: 37M05, 34F05, 92D30.

1. Introduction

In recent years, the re-emergence of vector-bone disease has become a global public health concern due to rapid urbanization, climate change, and increased human mobility. Among these diseases, the

Zika virus (ZIKV) has drawn significant attention owing to its rapid spread and severe neurological complication in new-borns. The Zika virus, a member of the Flaviviridae family, is primarily transmitted by the Aedes aegypti and Aedes albopictus mosquitoes, although alternative transmission routes such as sexual transmission have also been reported [32, 34]. First identified in Uganda in 1947, the virus remained largely neglected until major outbreaks occurred in the Pacific Islands, South America, and other tropical regions during 2015-2016 [32]. The infection is often asymptomatic or causes mild symptoms such as fever, rash, and joint pain, however, its association with microcephaly in infants and Guillain-Barre syndrome in adults has made it a disease of international concern. Understanding the transmission dynamics of Zika virus is therefore essential for predicting outbreaks and designing effective control strategies [32, 34].

Mathematical modelling plays a vital role in describing the dynamics of infectious diseases. It provides a framework to evaluate the effects of various biological and environmental factors on disease spread and persistence. Compartmental models, such as the classic SIR (Susceptible- Infected-Recovered) type, have been successfully used to analyse a wide range of diseases, including dengue, malaria, Ebola and Zika [7, 9, 24]. By extending these models with additional compartments or parameters, researchers can capture the specific biological processes relevant to each disease. Recent modelling efforts continue refining and expanding our understanding of Zika virus(ZIKV) dynamics-through more realistic assumptions, advanced mathematical techniques, and broader transmission pathways. Below are several representative studies [9, 33].

A notable contribution in this direction is the study " Numerical study for Zika virus transmission with Beddington-DeAngelis incidence rate" published in the Far East Journal of Mathematical Science (2019). In this work, the authors introduced a nonlinear Beddington-DeAngelis incidence function to model saturation effects in mosquito-human interactions. Their numerical analysis demonstrated that nonlinear incidence rate can significantly alter disease dynamics and prevent unrealistic exponential growth in transmission at high population densities [4].

More recently, numerical approaches have been widely employed to study Zika virus models where analytical solutions are difficult to obtain. The paper "Numerical Simulations and Solutions of a Mathematical Model for Zika Virus Disease" published in Applications of Modelling and Simulation (2025) focused on numerical approximation techniques to explore the behaviour of a Zika virus model involving human and mosquito populations. Their simulations highlighted the importance of mosquito lifespan, biting rate, and human recovery rate in controlling disease spread [14].

Another emerging area in Zika modelling is the use of fractional-order derivatives to incorporate memory and hereditary effects in disease transmission. The study "Optimal Control Problem for Mathematical Modelling of Zika Virus Transmission Using Fractional Order Derivatives" published in Frontiers in Applied Mathematics and Statistics (2024) formulated a fractional order Zika virus model using Caputo derivatives. The authors applied optimal control theory to investigate vaccination and vector control strategies, demonstrating that fractional models can capture long-term disease dynamics more effectively than classical integer-order models [19].

Co-infection modelling has also received attention due to the overlapping geographic distribution of vector-borne diseases. The paper "Modelling the Co-infection of Malaria and Zika Virus Disease" published in the Journal of the Nigerian Society of Physical Sciences (2024) developed a co-infection framework to study the interaction between malaria and Zika virus. Their analysis showed that co-

infection can increase disease burden and alter reproduction thresholds, emphasizing the importance of integrated disease management strategies in endemic regions [13].

Pregnancy-related transmission and maternal infection have been identified as critical aspects of Zika virus epidemiology. In this context, the study "Deterministic Model of Zika Virus with Carrier Mother and Reservoirs: A Mathematical Analysis Approach" published in the FUDMA Journal of Sciences (2023) introduced carrier mothers and reservoir populations into the modelling framework. Their analysis revealed that maternal carriers play a crucial role in sustaining disease transmission, even when overall infection levels appear low [11].

Between 2023 and 2025, several additional studies further expanded Zika virus modelling by incorporating seasonal variation, time delays, spatial heterogeneity, and advanced control strategies. Seasonal models demonstrated how fluctuations in mosquito populations influence outbreak periodicity, while delay differential equation models revealed the possibility of oscillatory outbreaks through Hopf bifurcation. Spatial reaction–diffusion models explored vector bias and Wolbachia-based mosquito control, showing promising results for disease elimination under appropriate conditions. These developments highlight the increasing sophistication of mathematical approaches used to study Zika virus dynamics [35, 33].

Despite these advances, several gaps remain in the existing literature. Many models do not explicitly include pregnant women as a separate epidemiological class or congenital infection compartments, which are essential for studying microcephaly risk and vertical transmission outcomes. Moreover, while numerical simulations are commonly used, few studies apply semi analytical methods that provide explicit approximate solutions and deeper insight into parameter dependencies. In particular, the q-Homotopy Analysis Transform Method (q-HATM) has not been widely applied to Zika virus models, despite its effectiveness in handling strongly nonlinear systems with adjustable convergence control [25, 27, 29, 30].

Motivated by these gaps, the present study proposes an extended deterministic Zika virus model that incorporates susceptible, exposed, infected, pregnant, congenital-infant, and recovered human populations, along with susceptible, exposed, and infected mosquito vectors. The model captures multiple transmission pathways, including mosquito-to-human infection and vertical transmission from infected pregnant women to infants. The basic reproduction number is derived using the next-generation matrix approach, and rigorous local and global stability analyses are performed for both disease-free and endemic equilibrium points [3, 9, 10, 24].

Optimal control provides a framework to determine the best allocation of resources to reduce infection in both human and vector populations [12, 20, 31]. To obtain approximate analytical solutions of the nonlinear system, the q-Homotopy Analysis Transform Method (q-HATM) is employed [1, 6, 15, 22, 23]. This method combines the Laplace transform with homotopy analysis and introduces an auxiliary convergence-control parameter, allowing accurate and convergent solutions without restrictive assumptions. Numerical simulations are presented to validate the analytical findings and to illustrate the effects of key parameters on Zika virus transmission dynamics.

The results of this study contribute to a deeper theoretical understanding of Zika virus epidemiology and provide a flexible mathematical framework that can be extended to include fractional dynamics, control strategies, or co-infection scenarios in future research. The findings may assist public health

authorities in designing effective intervention strategies to reduce Zika virus transmission and associated congenital complications.

2. MODEL FORMULATION

In this section, we formulate a deterministic compartmental model to describe the transmission dynamics of Zika virus between human and mosquito populations. The total population is divided into human and mosquito (vector) subpopulations, and disease transmission occurs through mosquito bites and vertical transmission. At time ι, the total human population is subdivided into the following compartments and initial values:

S_h : Susceptible humans =500

E_h : Exposed humans (infected but not yet infectious) =110

J_h : Infectious humans =75

P_h : Pregnant women infected with Zika virus =10

C_h : Congenitally infected infants =5

R_h : Recovered humans with immunity =10

Mosquito Population Structure : The mosquito population is divided into

S_{zv}: Susceptible mosquitoes =500

E_{zv} : Exposed mosquitoes =95

J_{zv} : Infected mosquitoes =70

Model Assumptions : The formulation of the model is based on the following assumptions:

Λ_h: Recruitment level of human into susceptible population =50

α: Biting rate of mosquitoes with Zika virus =0.4

η_1: Effective rate of transmission of Zika virus from mosquitoes to human =0.0009

ρ_1: Pregnancy rate from susceptible =0.07143

σ_p: Birth rate from infected pregnant women =0.6

ϵ: Fraction of new-born with congenital Zika =0.3

τ_1: Natural death rate of human =0.00004

δ: Rate of progression from exposed to infected =0.3333

ω: Rate of recovery =0.1429

τ_2: Disease induced death rate =0.0003

ν_c: Death rate of congenitally infected infant =0.03

Λ_{zv} : Recruitment level of aedes aegypti mosquitoes =100

η_2: Effective rate of transmission of Zika virus from infectious human to mosquitoes =0.07

κ: Mating rate of SIT mosquitoes with ades aegypti mosquitoes =0.5

Z_{SIT} : Population of sterile males to control aedes aegypti population =300

μ: Natural death rate of mosquitoes =0.0556

γ: Rate of development of exposed aedes aegypti mosquitoes to infectious aedes aegypti mosquitoes =0.1111.

2.1. Model Equations. Based on the above assumptions, the dynamics of the Zika virus transmission are governed by the following system of nonlinear ordinary differential equations.

Human Population Dynamics

$$\frac{dS_h}{d\iota} = \Lambda_h - \alpha\eta_1 J_{zv}(\iota)S_h(\iota) - \rho_1 S_h(\iota) + \sigma_p P_h(\iota) - \epsilon\sigma_p P_h(\iota) - \tau_1 S_h(\iota)$$

$$\frac{dE_h}{d\iota} = \alpha\eta_1 J_{zv}(\iota) S_h(\iota) - \delta E_h(\iota) - \tau_1 E_h(\iota)$$

$$\frac{dJ_h}{d\iota} = \delta E_h(\iota) - \omega J_h(\iota) - \tau_1 J_h(\iota) - \tau_2 J_h(\iota)$$

$$\frac{dP_h}{d\iota} = \rho_1 S_h(\iota) - \sigma_p P_h(\iota) - \rho_2 P_h(\iota) - \tau_1 P_h(\iota)$$

$$\frac{dC_h}{d\iota} = \epsilon\sigma_p P_h(\iota) - \nu_c C_h(\iota) - \tau_1 C_h(\iota)$$

$$\frac{dR_h}{d\iota} = \omega J_h(\iota) + \rho_2 P_h(\iota) + \nu_c C_h(\iota) - \tau_1 R_h(\iota) + \tau_2 J_h(\iota)$$

Mosquito Population Dynamics

$$\frac{dS_{zv}}{d\iota} = \Lambda_{zv} - \alpha\eta_2 J_h(\iota)S_{zv}(\iota) - \kappa Z_{SIT} S_{zv}(\iota) - \mu S_{zv}(\iota)$$

$$\frac{dE_{zv}}{d\iota} = \alpha\eta_2 J_h(\iota)S_{zv}(\iota) - \gamma E_{zv}(\iota) - \mu E_{zv}(\iota)$$

$$\frac{dJ_{zv}}{d\iota} = \gamma E_{zv}(\iota) - \mu J_{zv}(\iota).$$

(1)

3. Existence and Uniqueness of the Model Solutions

Theorem. 3.1. The functions defining the system (1) are continuous and satisfy the Lipschitz continuity condition with Lipschitz constants $Li \geq 0$, i= 1, 2, 3...9

Proof. Consider the nonlinear system (1) with initial conditions. Let the right hand side of the system be denoted by

$$f_1(\iota, S_h) = \Lambda_h - \alpha\eta_1 J_{zv}S_h - \rho_1 S_h + \sigma_p P_h - \epsilon\sigma_p P_h - \tau_1 S_h$$

$$f_2(\iota, E_h) = \alpha\eta_1 J_{zv} S_h - \delta E_h - \tau_1 E_h$$

$f_3(\iota, J_h) = \delta E_h - \omega J_h - \tau_1 J_h - \tau_2 J_h$

$f_4(\iota, P_h) = \rho_1 S_h - \sigma_p P_h - \rho_2 P_h - \tau_1 P_h$

$f_5(\iota, C_h) = \epsilon \sigma_p P_h - \nu_c C_h - \tau_1 C_h$

$f_6(\iota, R_h) = \omega J_h + \rho_2 P_h + \nu_c C_h - \tau_1 R_h + \tau_2 J_h$

$f_7(\iota, S_{zv}) = \Lambda_{zv} - \alpha \eta_2 J_h S_{zv} - \kappa Z_{SIT} S_{zv} - \mu S_{zv}$

$f_8(\iota, E_{zv}) = \alpha \eta_2 J_h S_{zv} - \gamma E_{zv} - \mu E_{zv}$

$f_9(\iota, J_{zv}) = \gamma E_{zv} - \mu J_{zv}$

Then the system can be written as

$\frac{dS_h}{d\iota} = f_1(\iota, S_h), \frac{dE_h}{d\iota} = f_2(\iota, E_h), \frac{dJ_h}{d\iota} = f_3(\iota, J_h), \frac{dP_h}{d\iota} = f_4(\iota, P_h), \frac{dC_h}{d\iota} = f_5(\iota, C_h), \frac{dR_h}{d\iota} = f_6(\iota, R_h)$

$\frac{dS_{zv}}{d\iota} = f_7(\iota, S_{zv}), \frac{dE_{zv}}{d\iota} = f_8(\iota, E_{zv}), \frac{dJ_{zv}}{d\iota} = f_9(\iota, J_{zv})$.

To prove the existence and uniqueness of solutions, we verify the Lipschitz condition.

Lipschitz condition for f_1 .

$$\begin{aligned} |f_1(\iota, S_h) - f_1(\iota, S_h^*)| &= |(\Lambda_h - \alpha \eta_1 J_{zv} S_h - \rho_1 S_h + \sigma_p P_h - \epsilon \sigma_p P_h - \tau_1 S_h) \\ &\quad \alpha \eta_1 J_{zv} S_h^* - \rho_1 S_h^* + \sigma_p S_h^* - \epsilon \sigma_p P_h - \tau_1 S_h^*)| \\ &= |(-\alpha \eta_1 J_{zv} - \rho_1 - \tau_1)(S_h - S_h^*)| \\ &= |(\alpha \eta_1 J_{zv} + \rho_1 + \tau_1)(S_h - S_h^*)| \end{aligned}$$

Thus,

$$|f_1(\iota, S_h) - f_1(\iota, S_h^*)| \leq L_1 |(S_h - S_h^*)|$$

Where

$$L_1 = |(\alpha \eta_1 J_{zv} + \rho_1 + \tau_1)|$$

The Lipschitz continuity with respect to S_h is established with L_1 as the Lipschitz constant. Similarly, the Lipschitz continuity with respect to the other state variables can be established in the same manner.

Where

$$|f_2(\iota, E_h) - f_2(\iota, E_h^*)| \leq L_2 |(E_h - E_h^*)|$$

$$|f_3(\iota, J_h) - f_3(\iota, J_h^*)| \leq L_3 |(J_h - J_h^*)|$$

$$|f_4(\iota, P_h) - f_4(\iota, P_h^*)| \leq L_4 |(P_h - P_h^*)|$$

$$|f_5(\iota, C_h) - f_5(\iota, C_h^*)| \leq L_5 |(C_h - C_h^*)|$$

$$|f_6(\iota, R_h) - f_6(\iota, R_h^*)| \leq L_6 |(R_h - R_h^*)|$$

$$|f_7(\iota, S_{zv}) - f_7(\iota, S_{zv}^*)| \leq L_7 |(S_{zv} - S_{zv}^*)|$$

$$|f_8(\iota, E_{zv}) - f_8(\iota, E_{zv}^*)| \leq L_8 |(E_{zv} - E_{zv}^*)|$$

$$|f_9(\iota, J_{zv}) - f_9(\iota, J^*_{zv})| \leq L_9 |(J_{zv} - J^*_{zv})|$$

where, $L_2 = |\delta + \tau_1|$, $L_3 = |\omega + \tau_1 + \tau_2|$, $L_4 = |\sigma_p + \rho_2 + \tau_1|$, $L_5 = |\nu_c + \tau_1|$, $L_6 = |\tau_1|$, $L_7 = |\alpha \eta_2 J_h + \kappa Z_{SIT} + \mu|$, $L_8 = |\gamma + \mu|$ and $L_9 = |\mu|$

Since the function f_1 , f_2, f_3 , f_4 , f_5 , f_6 , f_7, f_8 and f_9 are continuous and satisfy the Lipschitz condition, by the Picard- Lindelof theorem the system admits a unique solution for $\iota \geq 0$.

4. Stability Analysis and Equilibrium points

4.1. Local Stability. At the disease-free equilibrium (DFE), all infected compartments vanish. Thus, $E_h = J_h = P_h = C_h = E_{zv} = J_{zv} = R_h = 0$

4.1.1. Equilibrium Points. Disease-Free Equilibrium Setting the right-hand sides of the model equations equal to zero and substituting the infected compartments as zero, we obtain:

Human susceptible population: $\Lambda_h - (\rho_1 + \tau_1) S_h = 0$ and $S_h = \frac{\Lambda_h}{\rho_1 + \tau_1}$

Vector susceptible population: $\Lambda_{zv} - \kappa Z_{SIT} S_{zv} - \mu S_{zv} = 0$ and $S_{zv} = \frac{\Lambda_{zv}}{\kappa Z_{SIT} + \mu}$

Hence, the disease-free equilibrium point $E_0 = (\frac{\Lambda_h}{\rho_1 + \tau_1}, 0, 0, 0, 0, 0, \frac{\Lambda_{zv}}{\kappa Z_{SIT} + \mu}, 0, 0)$.

The Jacobian matrix evaluated at the DFE J (E_0) is:

$$J_0 = \begin{pmatrix} \boldsymbol{\partial_{11}} & 0 & 0 & 0 & 0 & 0 & 0 & 0 & \partial_{19} \\ 0 & \boldsymbol{\partial_{22}} & 0 & 0 & 0 & 0 & 0 & 0 & \partial_{29} \\ 0 & \partial_{32} & \boldsymbol{\partial_{33}} & 0 & 0 & 0 & 0 & 0 & 0 \\ \partial_{41} & 0 & 0 & \boldsymbol{\partial_{44}} & 0 & 0 & 0 & 0 & 0 \\ 0 & 0 & 0 & \partial_{54} & \boldsymbol{\partial_{55}} & 0 & 0 & 0 & 0 \\ 0 & 0 & \partial_{63} & \partial_{64} & \partial_{65} & \boldsymbol{\partial_{66}} & 0 & 0 & 0 \\ 0 & 0 & \partial_{73} & 0 & 0 & 0 & \boldsymbol{\partial_{77}} & 0 & 0 \\ 0 & 0 & \partial_{83} & 0 & 0 & 0 & 0 & \boldsymbol{\partial_{88}} & 0 \\ 0 & 0 & 0 & 0 & 0 & 0 & 0 & \partial_{98} & \boldsymbol{\partial_{99}} \end{pmatrix}$$

where $\boldsymbol{\partial_{11}} = -(\rho_1 + \tau_1)$, $\partial_{19} = -(\alpha \eta_1 S_h)$, $\boldsymbol{\partial_{22}} = -(\delta + \tau_1)$, $\partial_{29} = \alpha \eta_1 S_h$, $\partial_{32} = \delta$, $\boldsymbol{\partial_{33}} = -(\omega + \tau_1 + \tau_2)$, $\partial_{41} = \rho_1$, $\boldsymbol{\partial_{44}} = -(\sigma_p \rho_2 + \tau_1)$, $\partial_{54} = \epsilon \sigma_p$, $\boldsymbol{\partial_{55}} = -(\nu_c + \tau_1)$, $\partial_{63} = \omega$, $\partial_{64} = \rho_2$, $\partial_{65} = \nu_c$, $\boldsymbol{\partial_{66}} = -\tau_1$, $\partial_{73} = -(\alpha \eta_2 S_{zv})$, $\boldsymbol{\partial_{77}} = -(\kappa Z_{SIT} + \mu)$, $\partial_{83} = \alpha \eta_2 S_{zv}$ $\boldsymbol{\partial_{88}} = -(\gamma + \mu)$, $\partial_{98} = \gamma$, $\boldsymbol{\partial_{99}} = -\mu$.

Therefore, all the diagonal elements are negative by Routh - Hurwitz theorem DFE is locally stable.

4.1.2. Endemic Equilibrium points. For the endemic equilibrium point E^*

$S_h = \frac{(\delta + \tau_1)E_h}{\alpha \eta_1 J_{zv}}$, $E_h = \frac{\alpha \eta_1 J_{zv} S_h}{(\delta + \tau_1)}$, $J_h = \frac{\alpha \eta_1 J_{zv} S_h}{(\delta + \tau_1)(\omega + \tau_1 + \tau_2)}$, $P_h = \frac{\rho_1 S_h}{\sigma_p + \rho_2 + \tau_1|}$, $C_h = \frac{\epsilon \sigma_p P_h}{\nu_c + \tau_1}$,

$R_h = \frac{(\omega + \tau_1)J_h + \rho_2 P_h + \nu_c C_h}{\tau_1}$, $S_{zv} = \frac{\Lambda_{zv}}{\alpha \eta_2 J_h + \kappa Z_{SIT} + \mu}$, $E_{zv} = \frac{\alpha \eta_2 J_h S_{zv}}{\gamma + \mu}$, $J_{zv} = \frac{\alpha \eta_2 J_h S_{zv}}{(\gamma + \mu)\mu}$

By using endemic points in Jacobian J(E^*) all the main diagonal elements are still negative by Routh - Hurwitz theorem endemic equilibrium is stable.

4.2. Global Stability.

4.2.1. Disease-Free Equilibrium. Consider the Lyapunov function defined as

$V = E_h + J_h + P_h + C_h + E_{zv} + J_{zv}$.

Taking the derivative of V with respect to time along the solutions of the system gives

$$\frac{dV}{dt} = \frac{dE_h}{dt} + \frac{dJ_h}{dt} + \frac{dP_h}{dt} + \frac{dC_h}{dt} + \frac{dE_{zv}}{dt} + \frac{dJ_{zv}}{dt}.$$

Substituting the model equations yields

$$\frac{dV}{dt} = \alpha\eta_1 J_{zv} S_h + \alpha\eta_2 J_h S_{zv} - \tau_1 E_h - (\omega + \tau_1 + \tau_2) J_h - \mu E_{zv} - \mu J_{zv} + \rho_1 S_h - (\sigma_p + \rho_2 + \tau_1 - \epsilon\sigma_p) P_h - (\nu_c + \tau_1) C_h.$$

Since the population is bounded in the feasible region, we have

$S_h \leq S_h^*$, $S_{zv} \leq S_{zv}^*$.

$$\frac{dV}{dt} \leq \alpha\eta_1 J_{zv} S_h^* + \alpha\eta_2 J_h S_{zv}^* - \tau_1 E_h - (\omega + \tau_1 + \tau_2) J_h - \mu E_{zv} - \mu J_{zv} + \rho_1 S_h^* - (\sigma_p + \rho_2 + \tau_1 - \epsilon\sigma_p) P_h - (\nu_c + \tau_1) C_h.$$

Grouping the terms involving J_h and J_{zv} we obtain

$$\frac{dV}{dt} \leq (\alpha\eta_2 J_h S_{zv}^* - (\omega + \tau_1 + \tau_2) J_h + (\alpha\eta_1 S_h^* - \mu) J_{zv} - (\sigma_p + \rho_2 + \tau_1 - \epsilon\sigma_p) P_h - (\nu_c + \tau_1) C_h - \tau_1 E_h - \mu E_{zv}$$

Let the basic reproduction number be

$$R_0 = \sqrt{\frac{\alpha^2\eta_1\eta_2 S_h^* S_{zv}^*}{(\omega + \tau_1 + \tau_2)\mu}}$$

Then the derivative becomes

$$\frac{dV}{dt} \leq (\omega + \tau_1 + \tau_2)(R_0 - 1) J_h + \mu J_{zv}(R_0 - 1) - (\sigma_p + \rho_2 + \tau_1 - \epsilon\sigma_p) P_h - (\nu_c + \tau_1) C_h - \tau_1 E_h - \mu E_{zv}$$

If $R_0 \leq 1$, then

$$\frac{dV}{dt} \leq 0$$

The equality holds only when

$$E_h = J_h = P_h = C_h = E_{zv} = J_{zv} = 0.$$

Thus, by LaSalle's Invariance Principle, the disease-free equilibrium is globally asymptotically stable whenever $R_0 \leq 1$

4.2.2. Endemic Equilibrium. Assume that $R_0 > 1$. Let the endemic equilibrium be denoted by

$$E^* = (S_h^*,\ E_h^*,\ J_h^*,\ P_h^*,\ C_h^*,\ S_{zv}^*,\ E_{zv}^*,\ J_{zv}^*).$$

Consider the Lyapunov function

$$\begin{aligned} V = {} & S_h - S_h^* - S_h^* \ln\left(\frac{S_h}{S_h^*}\right) + E_h - E_h^* - E_h^* \ln\left(\frac{E_h}{E_h^*}\right) \\ & + J_h - J_h^* - J_h^* \ln\left(\frac{J_h}{J_h^*}\right) + P_h - P_h^* - P_h^* \ln\left(\frac{P_h}{P_h^*}\right) \\ & + C_h - C_h^* - C_h^* \ln\left(\frac{C_h}{C_h^*}\right) + S_{zv} - S_{zv}^* - S_{zv}^* \ln\left(\frac{S_{zv}}{S_{zv}^*}\right) \\ & + E_{zv} - E_{zv}^* - E_{zv}^* \ln\left(\frac{E_{zv}}{E_{zv}^*}\right) + J_{zv} - J_{zv}^* - J_{zv}^* \ln\left(\frac{J_{zv}}{J_{zv}^*}\right) \end{aligned}$$

Derivative of the Lyapunov function differentiating V with respect to time gives

$$\begin{aligned} \frac{dV}{dt} = {} & \left(1 - \frac{S_h^*}{S_h}\right)\frac{dS_h}{dt} + \left(1 - \frac{E_h^*}{E_h}\right)\frac{dE_h}{dt} + \left(1 - \frac{J_h^*}{J_h}\right)\frac{dJ_h}{dt} + \left(1 - \frac{P_h^*}{P_h}\right)\frac{dP_h}{dt} \\ & + \left(1 - \frac{C_h^*}{C_h}\right)\frac{dC_h}{dt} + \left(1 - \frac{S_{zv}^*}{S_{zv}}\right)\frac{dS_{zv}}{dt} + \left(1 - \frac{E_{zv}^*}{E_{zv}}\right)\frac{dE_{zv}}{dt} + \left(1 - \frac{J_{zv}^*}{J_{zv}}\right)\frac{dJ_{zv}}{dt} \end{aligned}$$

Substituting the model equations and using endemic equilibrium relations, we obtain

$$\begin{aligned} \frac{dV}{dt} = {} & \left(1 - \frac{S_h^*}{S_h}\right)[(\rho_1 + \tau_1 + \alpha\eta_1 J_{zv}^*)(S_h^* - S_h)] + \left(1 - \frac{E_h^*}{E_h}\right)[(\delta + \tau_1)(E_h^* - E_h)] \\ & + \left(1 - \frac{J_h^*}{J_h}\right)[(\omega + \tau_1 + \tau_2)(J_h^* - J_h)] + \left(1 - \frac{P_h^*}{P_h}\right)[(\sigma_p + \rho_2 + \tau_1)(P_h^* - P_h)] \\ & + \left(1 - \frac{C_h^*}{C_h}\right)[(\nu_c + \tau_1)(C_h^* - C_h)] + \left(1 - \frac{S_{zv}^*}{S_{zv}}\right)[\mu(S_{zv}^* - S_{zv}) + \alpha\eta_2(J_h^* S_{zv}^* - J_h S_{zv})] \\ & + \left(1 - \frac{E_{zv}^*}{E_{zv}}\right)[(\gamma + \mu)(E_{zv}^* - E_{zv})] + \left(1 - \frac{J_{zv}^*}{J_{zv}}\right)[\mu(J_{zv}^* - J_{zv})] \end{aligned}$$

Using the inequality

$$x - a - a\ln\left(\frac{x}{a}\right) \geq 0,$$

it follows that V is positive definite.

$$\frac{dV}{dt} = -\sum_{i=1}^{8} a_i \left(\frac{x_i}{x_i^*} - 1 - ln\frac{x_i}{x_i^*}\right)$$

Where $a_i > 0$ for $i = 1, 2, \ldots 8$, $(a_1 = \rho_1 + \tau_1,\ a_2 = \delta + \tau_1,\ a_3 = \omega + \tau_1 + \tau_2,\ a_4 = \rho_2 + \tau_1,\ a_5 = \nu_c + \tau_1,\ a_6 = \mu,\ a_7 = \gamma + \mu,\ a_8 = \mu)$.

for all x > 0, it follows that

$$\frac{dV}{dt} \leq 0$$

Thus, by LaSalle's invariance principle, the endemic equilibrium E^* is globally asymptotically stable.

5. Optimal Control Analysis

Mathematical models of infectious diseases can be used to evaluate the effectiveness of intervention strategies aimed at reducing disease transmission. Optimal control theory provides a framework for determining the best combination of control strategies that minimize disease burden while accounting for the cost of implementing such strategies.

In this study, optimal control theory is applied to determine the optimal levels of prevention, treatment, and vector control strategies that reduce the number of infected individuals in the human and vector populations.

We apply Pontryagin's Maximum Principle to derive the necessary conditions for optimal control of the system. Three time–dependent control functions $u_1(\iota)$, $u_2(\iota)$, and $u_3(\iota)$ are introduced into the model.

The controls satisfy the bounds

$$0 \leq u_1(\iota), u_2(\iota), u_3(\iota) \leq 1, \ \iota \in [0, T]$$

The control variables are defined as follows:

• $u_1(\iota)$ represents preventive measures that reduce disease transmission from infected vectors to susceptible humans.

• $u_2(\iota)$ represents treatment of infected individuals which reduces the infectious period.

• $u_3(\iota)$ represents vector control strategies such as mosquito population reduction or sterile insect technique.

Incorporating the control variables into the model, the controlled system becomes

$$\frac{dS_h}{d\iota} = \Lambda_h - \alpha \eta_1 J_{zv}(1 - u_1) S_h - \rho_1 S_h + \sigma_p P_h - \epsilon \sigma_p P_h - \tau_1 S_h$$

$$\frac{dE_h}{d\iota} = (1 - u_1) \alpha \eta_1 J_{zv} S_h - \delta E_h - \tau_1 E_h$$

$$\frac{dJ_h}{d\iota} = \delta E_h - (\omega + u_2) J_h - \tau_1 J_h - \tau_2 J_h$$

$$\frac{dP_h}{d\iota} = \rho_1 S_h - \sigma_p P_h - \rho_2 P_h - \tau_1 P_h$$

$$\frac{dC_h}{d\iota} = \epsilon \sigma_p P_h - \nu_c C_h - \tau_1 C_h$$

$$\frac{dR_h}{d\iota} = (\omega + u_2) J_h + \rho_2 P_h + \nu_c C_h - \tau_1 R_h + \tau_2 J_h$$

$$\frac{dS_{zv}}{d\iota} = \Lambda_{zv} - (1 - u_3) \alpha \eta_2 J_h S_{zv} - \kappa Z_{SIT} S_{zv} - \mu S_{zv}$$

$$\frac{dE_{zv}}{dt} = (1 - u_3)\,\alpha\,\eta_2\,J_h S_{zv} - \gamma\,E_{zv} - \mu\,E_{zv}$$

$$\frac{dJ_{zv}}{dt} = \gamma E_{zv} - \mu\,J_{zv}$$

The goal is to minimize the number of infected individuals and the cost associated with implementing the control strategies over the time interval [0, T].

$$J(u_1, u_2, u_3) = \int_0^T \left[A_1 J_h + A_2 J_{zv} + \frac{B_1}{2}u_1^2 + \frac{B_2}{2}u_2^2 + \frac{B_3}{2}u_3^2\right] dt$$

5.1. Existence of Optimal Control. Theorem. Given the objective functional and the controlled system with bounded controls, there exists an optimal control set $(\boldsymbol{u_1^*, u_2^*, u_3^*})$ and corresponding state variables that minimize the objective functional J (u_1,u_2,u_3). Furthermore, there exist adjoint variables $\lambda_i(t)$, i = 1, 2, . . . , 9, satisfying the adjoint system such that the optimal controls are characterized by the optimality conditions derived from Pontryagin's Maximum Principle.

The Hamiltonian function is defined as

$$\boldsymbol{H} = A_1 J_h + A_2 J_{zv} + \frac{B_1}{2}u_1^2 + \frac{B_2}{2}u_2^2 + \frac{B_3}{2}u_3^2 + \sum_{i=1}^{9}\lambda_i f_i$$

where λ_i are the adjoint variables and f_i represent the right-hand sides of the state equations. Where A_1 and A_2 are weight constants for infected individuals and vectors, while B_1, B_2, and B_3 represent the cost coefficients associated with the control measures.

The Hamiltonian function of our model,

$$\begin{aligned}\boldsymbol{H} = {} & A_1 J_h + A_2 J_{zv} + \frac{B_1}{2}u_1^2 + \frac{B_2}{2}u_2^2 + \frac{B_3}{2}u_3^2 \\ & + \lambda_1\left[\Lambda_h - \alpha\,\eta_1\,J_{zv}(1 - u_1)\,S_h - \rho_1\,S_h + \sigma_p\,P_h - \epsilon\,\sigma_p\,P_h - \tau_1\,S_h\right] \\ & + \lambda_2[(1 - u_1)\,\alpha\,\eta_1\,J_{zv}\,S_h - \delta\,E_h - \tau_1 E_h] \\ & + \lambda_3[\,\delta\,E_h - (\omega + u_2)\,J_h - \tau_1 J_h - \tau_2 J_h] \\ & + \lambda_4[\,\rho_1\,S_h - \sigma_p\,P_h - \rho_2\,P_h - \tau_1 P_h] \\ & + \lambda_5[\,\epsilon\,\sigma_p\,P_h - \nu_c\,C_h - \tau_1\,C_h] \\ & + \lambda_6[\,(\omega + u_2)\,J_h + \rho_2\,P_h + \nu_c\,C_h - \tau_1 R_h + \tau_2 J_h] \\ & + \lambda_7[\,\Lambda_{zv} - (1 - u_3)\,\alpha\,\eta_2\,J_h S_{zv} - \kappa\,Z_{SIT}\,S_{zv} - \mu\,S_{zv}] \\ & + \lambda_8[\,(1 - u_3)\,\alpha\,\eta_2\,J_h S_{zv} - \gamma\,E_{zv} - \mu\,E_{zv}] \\ & + \lambda_9[\,\gamma E_{zv} - \mu\,J_{zv}]\end{aligned}$$

where $\lambda_i(t)$, i = 1, 2, . . . , 9, are the adjoint variables corresponding to the state variables S_h, E_h, J_h, P_h, C_h, R_h, S_{zv}, E_{zv}, J_{zv} respectively. The adjoint variables satisfy

$$\frac{\boldsymbol{d}\lambda_i}{dt} = -\frac{\partial H}{\partial x_i}$$

for i = 1, 2, . . . , 9. Using Pontryagin's Maximum Principle, the adjoint variables $\lambda_i(\iota)$ satisfy the following system

$$\frac{d\lambda_1}{d\iota} = \lambda_1 [(1 - u_1)\,\alpha\,\eta_1\,J_{zv} + \rho_1 + \tau_1] - \lambda_2\,(1 - u_1)\,\alpha\,\eta_1\,J_{zv} - \lambda_4\,\rho_1$$

$$\frac{d\lambda_2}{d\iota} = \lambda_2\,(\delta + \tau_1) - \lambda_3\,\delta$$

$$\frac{d\lambda_3}{d\iota} = -A_1 + \lambda_3\,(\omega + u_2 + \tau_1 + \tau_2) - \lambda_6\,(\omega + u_2 + \tau_2) + \lambda_7\,(1 - u_3)\,\alpha\,\eta_2\,S_{zv} - \lambda_8\,(1 - u_3)\,\alpha\,\eta_2\,S_{zv}$$

$$\frac{d\lambda_4}{d\iota} = -\lambda_1\,\sigma_p + \lambda_1\,\epsilon\,\sigma_p + \lambda_4\,(\sigma_p + \rho_2 + \tau_1) - \lambda_5\epsilon\,\sigma_p - \lambda_6\,\rho_2$$

$$\frac{d\lambda_5}{d\iota} = \lambda_5\,(\nu_c + \tau_1) - \lambda_6\,\nu_c$$

$$\frac{d\lambda_6}{d\iota} = \lambda_6\,\tau_1$$

$$\frac{d\lambda_7}{d\iota} = \lambda_7[(1 - u_3)\alpha\,\eta_2 J_h + \kappa\,Z_{SIT} + \mu] - \lambda_8\,(1 - u_3)\,\alpha\,\eta_2 J_h$$

$$\frac{d\lambda_8}{d\iota} = \lambda_8\,(\gamma + \mu) - \lambda_9\gamma$$

$$\frac{d\lambda_9}{d\iota} = -A_2 + \lambda_1(1 - u_1)\,\alpha\,\eta_1 S_h - \lambda_2(1 - u_1)\,\alpha\,\eta_1 S_h + \lambda_9\,\mu$$

The adjoint variables satisfy the terminal conditions

$$\lambda_i(T) = 0,\ i = 1, 2, \ldots, 9$$

The optimal controls are obtained by solving

$$\frac{\partial H}{\partial u_i} = \mathbf{0}$$

which yields

$$u_1^* = min\left(1, max\left(0, \frac{\alpha\,\eta_1 S_h J_{zv}(\lambda_2 - \lambda_1)}{B_1}\right)\right)$$

$$u_2^* = min\left(1, max\left(0, \frac{J_h(\lambda_3 - \lambda_6)}{B_2}\right)\right)$$

$$u_3^* = min\left(1, max\left(0, \frac{\alpha\,\eta_2 S_{zv} J_h(\lambda_8 - \lambda_7)}{B_1}\right)\right)$$

In summary, the optimal control analysis provides a systematic framework to evaluate the effectiveness of prevention, treatment, and vector control strategies in reducing the burden of infection in both human and vector populations. By applying Pontryagin's Maximum Principle, we derived the necessary conditions for optimality in the form of adjoint equations, transversality conditions, and explicit expressions for the optimal control functions. The combined system of state and adjoint equations, together with the optimality conditions, forms a coupled forward–backward problem that can be solved numerically using standard techniques such as the forward–backward sweep method. This approach enables the identification of time-dependent intervention strategies that minimize the number of infections while accounting for the costs associated with implementing these measures, thereby providing valuable guidance for public health decision-making and disease management.

6. Application of the q− Homotopy Analysis Transform Method

In this section, we apply the q − Homotopy Analysis Transform Method to obtain approximate analytical solutions for the nonlinear Zika virus transmission model. The q−HATM combines the Laplace transform with the homotopy analysis method, providing a powerful and flexible framework for solving highly nonlinear systems of differential equations. For definition and properties of q−HATM one can refer [23, 25, 26, 29, 30, 31, 32]

The system (1) of fractional order equation,

$$D_\iota^\rho \mathrm{S_h}(\iota) = \Lambda_\mathrm{h} - \alpha\,\eta_1\,\mathrm{J_{zv}}(\iota)\mathrm{S_h}(\iota) - \rho_1\,\mathrm{S_h}(\iota) + \sigma_\mathrm{p}\,\mathrm{P_h}(\iota) - \epsilon\,\sigma_\mathrm{p}\,\mathrm{P_h}(\iota) - \tau_1\,\mathrm{S_h}(\iota)$$

$$D_\iota^\rho \mathrm{E_h}(\iota) = \alpha\,\eta_1\,\mathrm{J_{zv}}(\iota)\,\mathrm{S_h}(\iota) - \delta\,\mathrm{E_h}(\iota) - \tau_1\mathrm{E_h}(\iota)$$

$$D_\iota^\rho \mathrm{J_h}(\iota) = \delta\,\mathrm{E_h}(\iota) - \omega\,\mathrm{J_h}(\iota) - \tau_1\mathrm{J_h}(\iota) - \tau_2\mathrm{J_h}(\iota)$$

$$D_\iota^\rho \mathrm{P_h}(\iota) = \rho_1\,\mathrm{S_h}(\iota) - \sigma_\mathrm{p}\,\mathrm{P_h}(\iota) - \rho_2\,\mathrm{P_h}(\iota) - \tau_1\mathrm{P_h}(\iota)$$

$$D_\iota^\rho \mathrm{C_h}(\iota) = \epsilon\,\sigma_\mathrm{p}\,\mathrm{P_h}(\iota) - \nu_\mathrm{c}\,C_\mathrm{h}(\iota) - \tau_1\,C_\mathrm{h}(\iota)$$

$$D_\iota^\rho \mathrm{R_h}(\iota) = \omega\,\mathrm{J_h}(\iota) + \rho_2\,\mathrm{P_h}(\iota) + \nu_\mathrm{c}\,C_\mathrm{h}(\iota) - \tau_1 R_\mathrm{h}(\iota) + \tau_2\mathrm{J_h}(\iota)$$

$$D_\iota^\rho \mathrm{S_{zv}}(\iota) = \Lambda_\mathrm{zv} - \alpha\,\eta_2\,\mathrm{J_h}(\iota)\mathrm{S_{zv}}(\iota) - \kappa\,\mathrm{Z_{SIT}}\,\mathrm{S_{zv}}(\iota) - \mu\,\mathrm{S_{zv}}(\iota)$$

$$D_\iota^\rho \mathrm{E_{zv}}(\iota) = \alpha\,\eta_2\,\mathrm{J_h}(\iota)\mathrm{S_{zv}}(\iota) - \gamma\,\mathrm{E_{zv}}(\iota) - \mu\,\mathrm{E_{zv}}(\iota)$$

$$D_\iota^\rho \mathrm{J_{zv}}(\iota) = = \gamma\mathrm{E_{zv}}(\iota) - \mu\,\mathrm{J_{zv}}(\iota). \qquad (2)$$

We find the equation by applying the LT to system (1).

$$\mathrm{L}\{\mathrm{S_h}(\iota)\} - \frac{1}{\mathrm{s}}\,\mathrm{S_{h0}} - \frac{1}{\mathrm{B}(\wp)}\left(1 - \wp + \frac{\wp}{S^\wp}\right) + \mathrm{L}\{\Lambda_\mathrm{h} - \alpha\,\eta_1\,\mathrm{J_{zv}}(\iota)\mathrm{S_h}(\iota) - \rho_1\,\mathrm{S_h}(\iota) + \sigma_\mathrm{p}\,\mathrm{P_h}(\iota) - \epsilon\,\sigma_\mathrm{p}\,\mathrm{P_h}(\iota) - \tau_1\,\mathrm{S_h}(\iota)\} = 0$$

$$\mathrm{L}\{\mathrm{E_h}(\iota)\} - \frac{1}{\mathrm{s}}\,\mathrm{E_{h0}} - \frac{1}{\mathrm{B}(\wp)}\left(1 - \wp + \frac{\wp}{S^\wp}\right) + L\{\alpha\,\eta_1\,\mathrm{J_{zv}}(\iota)\mathrm{S_h}(\iota) - \delta\,\mathrm{E_h}(\iota) - \tau_1\mathrm{E_h}(\iota)\} = 0$$

$$\mathrm{L}\{\mathrm{J_h}(\iota)\} - \frac{1}{\mathrm{s}}\,\mathrm{J_{h0}} - \frac{1}{\mathrm{B}(\wp)}\left(1 - \wp + \frac{\wp}{S^\wp}\right) + L\{\delta\,\mathrm{E_h}(\iota) - \omega\,\mathrm{J_h}(\iota) - \tau_1\mathrm{J_h}(\iota) - \tau_2\mathrm{J_h}(\iota)\} = 0$$

$$\mathrm{L}\{P_\mathrm{h}(\iota)\} - \frac{1}{\mathrm{s}}\,P_{\mathrm{h0}} - \frac{1}{\mathrm{B}(\wp)}\left(1 - \wp + \frac{\wp}{S^\wp}\right) + L\{\rho_1\,\mathrm{S_h}(\iota) - \sigma_\mathrm{p}\,\mathrm{P_h}(\iota) - \rho_2\,\mathrm{P_h}(\iota) - \tau_1\mathrm{P_h}(\iota)\} = 0$$

$$\mathrm{L}\{\mathrm{C_h}(\iota)\} - \frac{1}{\mathrm{s}}\,\mathrm{C_{h0}} - \frac{1}{\mathrm{B}(\wp)}\left(1 - \wp + \frac{\wp}{S^{\wp}}\right) + L\{\epsilon\,\sigma_{\mathrm{p}}\,\mathrm{P_h}(\iota) - \nu_{\mathrm{c}}\,C_{\mathrm{h}}(\iota) - \tau_1\,C_{\mathrm{h}}(\iota)\} = 0$$

$$\mathrm{L}\{\mathrm{R_h}(\iota)\} - \frac{1}{\mathrm{s}}\,\mathrm{R_{h0}} - \frac{1}{\mathrm{B}(\wp)}\left(1 - \wp + \frac{\wp}{S^{\wp}}\right) + L\{\omega\,\mathrm{J_h}(\iota) + \rho_2\,\mathrm{P_h}(\iota) + \nu_{\mathrm{c}}\,C_{\mathrm{h}}(\iota) - \tau_1 R_{\mathrm{h}}(\iota) + \tau_2 \mathrm{J_h}(\iota)\} = 0$$

$$\mathrm{L}\{\mathrm{S_{zv}}(\iota)\} - \frac{1}{\mathrm{s}}\,\mathrm{S_{zv0}} - \frac{1}{\mathrm{B}(\wp)}\left(1 - \wp + \frac{\wp}{S^{\wp}}\right) + \mathrm{L}\{\Lambda_{\mathrm{zv}} - \alpha\,\eta_2\,\mathrm{J_h}(\iota)\mathrm{S_{zv}}(\iota) - \kappa\,\mathrm{Z_{SIT}}\,\mathrm{S_{zv}}(\iota) - \mu\,\mathrm{S_{zv}}(\iota)\} = 0$$

$$\mathrm{L}\{\mathrm{E_{zv}}(\iota)\} - \frac{1}{\mathrm{s}}\,\mathrm{E_{zv0}} - \frac{1}{\mathrm{B}(\wp)}\left(1 - \wp + \frac{\wp}{S^{\wp}}\right) + L\{\alpha\,\eta_2\,\mathrm{J_h}(\iota)\mathrm{S_{zv}}(\iota) - \gamma\,\mathrm{E_{zv}}(\iota) - \mu\,\mathrm{E_{zv}}(\iota)\} = 0$$

$$\mathrm{L}\{\mathrm{J_{zv}}(\iota)\} - \frac{1}{\mathrm{s}}\,\mathrm{J_{zv0}} - \frac{1}{\mathrm{B}(\wp)}\left(1 - \wp + \frac{\wp}{S^{\wp}}\right) + L\{\gamma \mathrm{E_{zv}}(\iota) - \mu\,\mathrm{J_{zv}}(\iota)\} = 0 \qquad (3)$$

Next, using a non-linear operator, we obtain

$$\mathrm{N}^1[\vartheta_1,\vartheta_2,\vartheta_3,\vartheta_4,\vartheta_5,\vartheta_6,\vartheta_7,\vartheta_8,\vartheta_9] = \mathrm{L}\{\vartheta_1(\iota;\,\mathrm{q})\} - \frac{1}{\mathrm{s}}\,\mathrm{S_{h0}} - \frac{1}{\mathrm{B}(\wp)}\left(1 - \wp + \frac{\wp}{S^{\wp}}\right) \times \mathrm{L}\{\Lambda_{\mathrm{h}} - \alpha\,\eta_1\vartheta_1(\iota;\,\mathrm{q})\vartheta_9(\iota;\,\mathrm{q}) - \rho_1\,\vartheta_1(\iota;\,\mathrm{q}) + (1-\epsilon)\sigma_{\mathrm{p}}\,\vartheta_4(\iota;\,\mathrm{q}) - \tau_1\vartheta_1(\iota;\,\mathrm{q})\},$$

$$\mathrm{N}^2[\vartheta_1,\vartheta_2,\vartheta_3,\vartheta_4,\vartheta_5,\vartheta_6,\vartheta_7,\vartheta_8,\vartheta_9] = \mathrm{L}\{\vartheta_2(\iota;\,\mathrm{q})\} - \frac{1}{\mathrm{s}}\,\mathrm{E_{h0}} - \frac{1}{\mathrm{B}(\wp)}\left(1 - \wp + \frac{\wp}{S^{\wp}}\right) \times \mathrm{L}\{\alpha\,\eta_1\vartheta_1(\iota;\,\mathrm{q})\,\vartheta_9(\iota;\,\mathrm{q}) - (\delta + \tau_1)\,\vartheta_2(\iota;\,\mathrm{q})\},$$

$$\mathrm{N}^3[\vartheta_1,\vartheta_2,\vartheta_3,\vartheta_4,\vartheta_5,\vartheta_6,\vartheta_7,\vartheta_8,\vartheta_9] = \mathrm{L}\{\vartheta_3(\iota;\,\mathrm{q})\} - \frac{1}{\mathrm{s}}\,\mathrm{J_{h0}} - \frac{1}{\mathrm{B}(\wp)}\left(1 - \wp + \frac{\wp}{S^{\wp}}\right) \times \mathrm{L}\{\delta\vartheta_2(\iota;\,\mathrm{q}) - (\omega + \tau_1 + \tau_2)\,\vartheta_3(\iota;\,\mathrm{q})\},$$

$$\mathrm{N}^4[\vartheta_1,\vartheta_2,\vartheta_3,\vartheta_4,\vartheta_5,\vartheta_6,\vartheta_7,\vartheta_8,\vartheta_9] = \mathrm{L}\{\vartheta_4(\iota;\,\mathrm{q})\} - \frac{1}{\mathrm{s}}\,\mathrm{P_{h0}} - \frac{1}{\mathrm{B}(\wp)}\left(1 - \wp + \frac{\wp}{S^{\wp}}\right) \times \mathrm{L}\{\rho_1\,\vartheta_1(\iota;\,\mathrm{q}) - (\sigma_{\mathrm{p}} + \rho_2 + \tau_1)\,\vartheta_4(\iota;\,\mathrm{q})\},$$

$$\mathrm{N}^5[\vartheta_1,\vartheta_2,\vartheta_3,\vartheta_4,\vartheta_5,\vartheta_6,\vartheta_7,\vartheta_8,\vartheta_9] = \mathrm{L}\{\vartheta_5(\iota;\,\mathrm{q})\} - \frac{1}{\mathrm{s}}\,\mathrm{C_{h0}} - \frac{1}{\mathrm{B}(\wp)}\left(1 - \wp + \frac{\wp}{S^{\wp}}\right) \times \mathrm{L}\{\epsilon\sigma_{\mathrm{p}}\,\vartheta_4(\iota;\,\mathrm{q}) - (\nu_{\mathrm{c}} + \tau_1)\,\vartheta_5(\iota;\,\mathrm{q})\},$$

$$\mathrm{N}^6[\vartheta_1,\vartheta_2,\vartheta_3,\vartheta_4,\vartheta_5,\vartheta_6,\vartheta_7,\vartheta_8,\vartheta_9] = \mathrm{L}\{\vartheta_6(\iota;\,\mathrm{q})\} - \frac{1}{\mathrm{s}}\,\mathrm{R_{h0}} - \frac{1}{\mathrm{B}(\wp)}\left(1 - \wp + \frac{\wp}{S^{\wp}}\right) \times \mathrm{L}\{\omega\vartheta_3(\iota;\,\mathrm{q}) + \rho_2\,\vartheta_4(\iota;\,\mathrm{q}) + \nu_{\mathrm{c}}\vartheta_5(\iota;\,\mathrm{q}) + \tau_2\vartheta_3(\iota;\,\mathrm{q}) - \tau_1\vartheta_6(\iota;\,\mathrm{q})\},$$

$$\mathrm{N}^7[\vartheta_1,\vartheta_2,\vartheta_3,\vartheta_4,\vartheta_5,\vartheta_6,\vartheta_7,\vartheta_8,\vartheta_9] = \mathrm{L}\{\vartheta_7(\iota;\,\mathrm{q})\} - \frac{1}{\mathrm{s}}\,\mathrm{S_{zv0}} - \frac{1}{\mathrm{B}(\wp)}\left(1 - \wp + \frac{\wp}{S^{\wp}}\right) \times \mathrm{L}\{\Lambda_{\mathrm{zv}} - \alpha\,\eta_2\,\vartheta_7(\iota;\,\mathrm{q})\vartheta_3(\iota;\,\mathrm{q}) - (\kappa\,\mathrm{Z_{SIT}} + \mu)\vartheta_7(\iota;\,\mathrm{q})\},$$

$$\mathrm{N}^8[\vartheta_1,\vartheta_2,\vartheta_3,\vartheta_4,\vartheta_5,\vartheta_6,\vartheta_7,\vartheta_8,\vartheta_9] = \mathrm{L}\{\vartheta_8(\iota;\,\mathrm{q})\} - \frac{1}{\mathrm{s}}\,E_{\mathrm{zv0}} - \frac{1}{\mathrm{B}(\wp)}\left(1 - \wp + \frac{\wp}{S^{\wp}}\right) \times \mathrm{L}\{\alpha\,\eta_2\,\vartheta_7(\iota;\,\mathrm{q})\vartheta_3(\iota;\,\mathrm{q}) - (\gamma + \mu)\,\vartheta_8(\iota;\,\mathrm{q})\},$$

$$\mathrm{N}^9[\vartheta_1,\vartheta_2,\vartheta_3,\vartheta_4,\vartheta_5,\vartheta_6,\vartheta_7,\vartheta_8,\vartheta_9] = \mathrm{L}\{\vartheta_9(\iota;\,\mathrm{q})\} - \frac{1}{\mathrm{s}}\,\mathrm{J_{zv0}} - \frac{1}{\mathrm{B}(\wp)}\left(1 - \wp + \frac{\wp}{S^{\wp}}\right) \times \mathrm{L}\{\gamma\,\vartheta_8(\iota;\,\mathrm{q}) - \mu\,\vartheta_9(\iota;\,\mathrm{q})\}. \qquad (4)$$

The r^{th} order deformation equation for H(x, ι) = 1 is given as

$$\mathrm{L}\left[\mathrm{S}_{\mathrm{h_r}}(\iota) - \mathrm{K_r}\mathrm{S}_{\mathrm{h_{r-1}}}(\iota)\right] = \mathrm{h}\,\Re_{1,\mathrm{r}}\left[\vec{\mathrm{S}}_{\mathrm{h_{r-1}}}, \vec{\mathrm{E}}_{\mathrm{h_{r-1}}}, \vec{\mathrm{J}}_{\mathrm{h_{r-1}}}, \vec{\mathrm{P}}_{\mathrm{h_{r-1}}}, \vec{\mathrm{C}}_{\mathrm{h_{r-1}}}, \vec{\mathrm{R}}_{\mathrm{h_{r-1}}}, \vec{\mathrm{S}}_{\mathrm{zv_{r-1}}}, \vec{\mathrm{E}}_{\mathrm{zv_{r-1}}}, \vec{\mathrm{J}}_{\mathrm{zv_{r-1}}}\right]$$

$$\mathrm{L}\left[\mathrm{E}_{\mathrm{h_r}}(\iota) - \mathrm{K_r}\mathrm{E}_{\mathrm{h_{r-1}}}(\iota)\right] = \mathrm{h}\,\Re_{2,\mathrm{r}}\left[\vec{\mathrm{S}}_{\mathrm{h_{r-1}}}, \vec{\mathrm{E}}_{\mathrm{h_{r-1}}}, \vec{\mathrm{J}}_{\mathrm{h_{r-1}}}, \vec{\mathrm{P}}_{\mathrm{h_{r-1}}}, \vec{\mathrm{C}}_{\mathrm{h_{r-1}}}, \vec{\mathrm{R}}_{\mathrm{h_{r-1}}}, \vec{\mathrm{S}}_{\mathrm{zv_{r-1}}}, \vec{\mathrm{E}}_{\mathrm{zv_{r-1}}}, \vec{\mathrm{J}}_{\mathrm{zv_{r-1}}}\right]$$

$$\mathrm{L}\left[\mathrm{J}_{\mathrm{h_r}}(\iota) - \mathrm{K_r}\mathrm{J}_{\mathrm{h_{r-1}}}(\iota)\right] = \mathrm{h}\,\Re_{3,\mathrm{r}}\left[\vec{\mathrm{S}}_{\mathrm{h_{r-1}}}, \vec{\mathrm{E}}_{\mathrm{h_{r-1}}}, \vec{\mathrm{J}}_{\mathrm{h_{r-1}}}, \vec{\mathrm{P}}_{\mathrm{h_{r-1}}}, \vec{\mathrm{C}}_{\mathrm{h_{r-1}}}, \vec{\mathrm{R}}_{\mathrm{h_{r-1}}}, \vec{\mathrm{S}}_{\mathrm{zv_{r-1}}}, \vec{\mathrm{E}}_{\mathrm{zv_{r-1}}}, \vec{\mathrm{J}}_{\mathrm{zv_{r-1}}}\right]$$

$$\mathrm{L}\left[\mathrm{P}_{\mathrm{h_r}}(\iota) - \mathrm{K_r}\mathrm{P}_{\mathrm{h_{r-1}}}(\iota)\right] = \mathrm{h}\,\Re_{4,\mathrm{r}}\left[\vec{\mathrm{S}}_{\mathrm{h_{r-1}}}, \vec{\mathrm{E}}_{\mathrm{h_{r-1}}}, \vec{\mathrm{J}}_{\mathrm{h_{r-1}}}, \vec{\mathrm{P}}_{\mathrm{h_{r-1}}}, \vec{\mathrm{C}}_{\mathrm{h_{r-1}}}, \vec{\mathrm{R}}_{\mathrm{h_{r-1}}}, \vec{\mathrm{S}}_{\mathrm{zv_{r-1}}}, \vec{\mathrm{E}}_{\mathrm{zv_{r-1}}}, \vec{\mathrm{J}}_{\mathrm{zv_{r-1}}}\right]$$

$$\mathrm{L}\left[\mathrm{C}_{\mathrm{h_r}}(\iota) - \mathrm{K_r}\mathrm{C}_{\mathrm{h_{r-1}}}(\iota)\right] = \mathrm{h}\,\Re_{5,\mathrm{r}}\left[\vec{\mathrm{S}}_{\mathrm{h_{r-1}}}, \vec{\mathrm{E}}_{\mathrm{h_{r-1}}}, \vec{\mathrm{J}}_{\mathrm{h_{r-1}}}, \vec{\mathrm{P}}_{\mathrm{h_{r-1}}}, \vec{\mathrm{C}}_{\mathrm{h_{r-1}}}, \vec{\mathrm{R}}_{\mathrm{h_{r-1}}}, \vec{\mathrm{S}}_{\mathrm{zv_{r-1}}}, \vec{\mathrm{E}}_{\mathrm{zv_{r-1}}}, \vec{\mathrm{J}}_{\mathrm{zv_{r-1}}}\right]$$

$$\mathrm{L}\left[\mathrm{R}_{\mathrm{h_r}}(\iota) - \mathrm{K_r}\mathrm{R}_{\mathrm{h_{r-1}}}(\iota)\right] = \mathrm{h}\,\Re_{6,\mathrm{r}}\left[\vec{\mathrm{S}}_{\mathrm{h_{r-1}}}, \vec{\mathrm{E}}_{\mathrm{h_{r-1}}}, \vec{\mathrm{J}}_{\mathrm{h_{r-1}}}, \vec{\mathrm{P}}_{\mathrm{h_{r-1}}}, \vec{\mathrm{C}}_{\mathrm{h_{r-1}}}, \vec{\mathrm{R}}_{\mathrm{h_{r-1}}}, \vec{\mathrm{S}}_{\mathrm{zv_{r-1}}}, \vec{\mathrm{E}}_{\mathrm{zv_{r-1}}}, \vec{\mathrm{J}}_{\mathrm{zv_{r-1}}}\right]$$

$$\mathrm{L}\left[\mathrm{S}_{\mathrm{zv_r}}(\iota) - \mathrm{K_r}\mathrm{S}_{\mathrm{zv_{r-1}}}(\iota)\right] = \mathrm{h}\,\Re_{7,\mathrm{r}}\left[\vec{\mathrm{S}}_{\mathrm{h_{r-1}}}, \vec{\mathrm{E}}_{\mathrm{h_{r-1}}}, \vec{\mathrm{J}}_{\mathrm{h_{r-1}}}, \vec{\mathrm{P}}_{\mathrm{h_{r-1}}}, \vec{\mathrm{C}}_{\mathrm{h_{r-1}}}, \vec{\mathrm{R}}_{\mathrm{h_{r-1}}}, \vec{\mathrm{S}}_{\mathrm{zv_{r-1}}}, \vec{\mathrm{E}}_{\mathrm{zv_{r-1}}}, \vec{\mathrm{J}}_{\mathrm{zv_{r-1}}}\right]$$

$$\mathrm{L}\left[\mathrm{E}_{\mathrm{zv_r}}(\iota) - \mathrm{K_r}\mathrm{E}_{\mathrm{zv_{r-1}}}(\iota)\right] = \mathrm{h}\,\Re_{8,\mathrm{r}}\left[\vec{\mathrm{S}}_{\mathrm{h_{r-1}}}, \vec{\mathrm{E}}_{\mathrm{h_{r-1}}}, \vec{\mathrm{J}}_{\mathrm{h_{r-1}}}, \vec{\mathrm{P}}_{\mathrm{h_{r-1}}}, \vec{\mathrm{C}}_{\mathrm{h_{r-1}}}, \vec{\mathrm{R}}_{\mathrm{h_{r-1}}}, \vec{\mathrm{S}}_{\mathrm{zv_{r-1}}}, \vec{\mathrm{E}}_{\mathrm{zv_{r-1}}}, \vec{\mathrm{J}}_{\mathrm{zv_{r-1}}}\right]$$

$$\mathrm{L}\left[\mathrm{J}_{\mathrm{h_r}}(\iota) - \mathrm{K_r}\mathrm{J}_{\mathrm{h_{r-1}}}(\iota)\right] = \mathrm{h}\,\Re_{9,\mathrm{r}}\left[\vec{\mathrm{S}}_{\mathrm{h_{r-1}}}, \vec{\mathrm{E}}_{\mathrm{h_{r-1}}}, \vec{\mathrm{J}}_{\mathrm{h_{r-1}}}, \vec{\mathrm{P}}_{\mathrm{h_{r-1}}}, \vec{\mathrm{C}}_{\mathrm{h_{r-1}}}, \vec{\mathrm{R}}_{\mathrm{h_{r-1}}}, \vec{\mathrm{S}}_{\mathrm{zv_{r-1}}}, \vec{\mathrm{E}}_{\mathrm{zv_{r-1}}}, \vec{\mathrm{J}}_{\mathrm{zv_{r-1}}}\right]$$

(5)

where,

$$\Re_{1,\mathrm{r}}\left[\vec{\mathrm{S}}_{\mathrm{h_{r-1}}}, \vec{\mathrm{E}}_{\mathrm{h_{r-1}}}, \vec{\mathrm{J}}_{\mathrm{h_{r-1}}}, \vec{\mathrm{P}}_{\mathrm{h_{r-1}}}, \vec{\mathrm{C}}_{\mathrm{h_{r-1}}}, \vec{\mathrm{R}}_{\mathrm{h_{r-1}}}, \vec{\mathrm{S}}_{\mathrm{zv_{r-1}}}, \vec{\mathrm{E}}_{\mathrm{zv_{r-1}}}, \vec{\mathrm{J}}_{\mathrm{zv_{r-1}}}\right] = \mathrm{L}\{\mathrm{S}_{\mathrm{h_{r-1}}}(\iota)\} - \left(1 - \frac{\mathrm{Kr}}{n}\right)\frac{S_{h_0}}{s} - \frac{1}{\mathrm{B}(\wp)}\left(1 - \wp + \frac{\wp}{S^{\wp}}\right) \times L\{\alpha\,\eta_1 \sum_{i=0}^{r-1} S_{h_i}(\iota) J_{h_{r-1-i}}(\iota) - \rho_1 S_{h_{r-1}}(\iota) + \sigma_{\mathrm{p}} P_{h_{r-1}}(\iota) - \epsilon\sigma_{\mathrm{p}} P_{h_{r-1}}(\iota) - \tau_1 S_{h_{r-1}}(\iota)\}$$

$$\Re_{2,\mathrm{r}}\left[\vec{\mathrm{S}}_{\mathrm{h_{r-1}}}, \vec{\mathrm{E}}_{\mathrm{h_{r-1}}}, \vec{\mathrm{J}}_{\mathrm{h_{r-1}}}, \vec{\mathrm{P}}_{\mathrm{h_{r-1}}}, \vec{\mathrm{C}}_{\mathrm{h_{r-1}}}, \vec{\mathrm{R}}_{\mathrm{h_{r-1}}}, \vec{\mathrm{S}}_{\mathrm{zv_{r-1}}}, \vec{\mathrm{E}}_{\mathrm{zv_{r-1}}}, \vec{\mathrm{J}}_{\mathrm{zv_{r-1}}}\right] = \mathrm{L}\{\mathrm{E}_{\mathrm{h_{r-1}}}(\iota)\} - \left(1 - \frac{\mathrm{Kr}}{n}\right)\frac{E_{h_0}}{s} - \frac{1}{\mathrm{B}(\wp)}\left(1 - \wp + \frac{\wp}{S^{\wp}}\right) \times L\{\alpha\,\eta_1 \sum_{i=0}^{r-1} S_{h_i}(\iota) J_{h_{r-1-i}}(\iota) - (\delta + \tau_1) E_{h_{r-1}}(\iota)\}$$

$$\Re_{3,\mathrm{r}}\left[\vec{\mathrm{S}}_{\mathrm{h_{r-1}}}, \vec{\mathrm{E}}_{\mathrm{h_{r-1}}}, \vec{\mathrm{J}}_{\mathrm{h_{r-1}}}, \vec{\mathrm{P}}_{\mathrm{h_{r-1}}}, \vec{\mathrm{C}}_{\mathrm{h_{r-1}}}, \vec{\mathrm{R}}_{\mathrm{h_{r-1}}}, \vec{\mathrm{S}}_{\mathrm{zv_{r-1}}}, \vec{\mathrm{E}}_{\mathrm{zv_{r-1}}}, \vec{\mathrm{J}}_{\mathrm{zv_{r-1}}}\right] = \mathrm{L}\{\mathrm{J}_{\mathrm{h_{r-1}}}(\iota)\} - \left(1 - \frac{\mathrm{Kr}}{n}\right)\frac{J_{h_0}}{s} - \frac{1}{\mathrm{B}(\wp)}\left(1 - \wp + \frac{\wp}{S^{\wp}}\right) \times L\{\delta \mathrm{E}_{\mathrm{h_{r-1}}}(\iota) - (\omega + \tau_1 + \tau_2)\mathrm{J}_{\mathrm{h_{r-1}}}(\iota)\}$$

$$\mathfrak{R}_{4,r}\left[\vec{S}_{h_{r-1}},\ \vec{E}_{h_{r-1}},\vec{J}_{h_{r-1}},\ \vec{P}_{h_{r-1}},\ \vec{C}_{h_{r-1}},\ \vec{R}_{h_{r-1}},\ \vec{S}_{zv_{r-1}},\vec{E}_{zv_{r-1}},\ \vec{J}_{zv_{r-1}},\right]=\ \mathrm{L}\{\mathrm{P}_{h_{r-1}}(\iota)\}$$
$$-\left(1-\frac{\mathrm{Kr}}{n}\right)\frac{P_{h_0}}{s}-\frac{1}{\mathrm{B}(\wp)}\left(1-\wp+\frac{\wp}{S^{\wp}}\right)\times L\{\ \rho_1 S_{h_{r-1}}(\iota)-(\sigma_{\mathrm{p}}+\rho_2+\tau_1)\mathrm{P}_{h_{r-1}}(\iota)\}$$

$$\mathfrak{R}_{5,r}\left[\vec{S}_{h_{r-1}},\ \vec{E}_{h_{r-1}},\vec{J}_{h_{r-1}},\ \vec{P}_{h_{r-1}},\ \vec{C}_{h_{r-1}},\ \vec{R}_{h_{r-1}},\ \vec{S}_{zv_{r-1}},\vec{E}_{zv_{r-1}},\ \vec{J}_{zv_{r-1}},\right]=\ \mathrm{L}\{\mathrm{C}_{h_{r-1}}(\iota)\}$$
$$-\left(1-\frac{\mathrm{Kr}}{n}\right)\frac{C_{h_0}}{s}-\frac{1}{\mathrm{B}(\wp)}\left(1-\wp+\frac{\wp}{S^{\wp}}\right)\times L\{\ \epsilon\sigma_{\mathrm{p}}P_{h_{r-1}}(\iota)-(\nu_{\mathrm{c}}+\tau_1)C_{h_{r-1}}(\iota)\}$$

$$\mathfrak{R}_{6,r}\left[\vec{S}_{h_{r-1}},\ \vec{E}_{h_{r-1}},\vec{J}_{h_{r-1}},\ \vec{P}_{h_{r-1}},\ \vec{C}_{h_{r-1}},\ \vec{R}_{h_{r-1}},\ \vec{S}_{zv_{r-1}},\vec{E}_{zv_{r-1}},\ \vec{J}_{zv_{r-1}},\right]=\ \mathrm{L}\{\mathrm{R}_{h_{r-1}}(\iota)\}$$
$$-\left(1-\frac{\mathrm{Kr}}{n}\right)\frac{R_{h_0}}{s}-\frac{1}{\mathrm{B}(\wp)}\left(1-\wp+\frac{\wp}{S^{\wp}}\right)\times L\{\ \omega\mathrm{J}_{h_{r-1}}(\iota)+\rho_2\,P_{h_{r-1}}(\iota)+\nu_{\mathrm{c}}\,\mathrm{C}_{h_{r-1}}(\iota)-\tau_1 R_{h_{r-1}}(\iota)+$$
$$\tau_2\mathrm{J}_{h_{r-1}}(\iota)\}$$

$$\mathfrak{R}_{7,r}\left[\vec{S}_{h_{r-1}},\ \vec{E}_{h_{r-1}},\vec{J}_{h_{r-1}},\ \vec{P}_{h_{r-1}},\ \vec{C}_{h_{r-1}},\ \vec{R}_{h_{r-1}},\ \vec{S}_{zv_{r-1}},\vec{E}_{zv_{r-1}},\ \vec{J}_{zv_{r-1}},\right]=\ \mathrm{L}\{\mathrm{S}_{zv_{r-1}}(\iota)\}$$
$$-\left(1-\frac{\mathrm{Kr}}{n}\right)\frac{S_{zv_0}}{s}-\frac{1}{\mathrm{B}(\wp)}\left(1-\wp+\frac{\wp}{S^{\wp}}\right)\times L\{\ \Lambda_{\mathrm{zv}}-\alpha\,\eta_2\sum_{i=0}^{r-1}S_{zv_{r-1-i}}(\iota)J_{h_i}(\iota)-(\kappa\,\mathrm{Z}_{\mathrm{SIT}}+$$
$$\mu)S_{zv_{r-1}}(\iota)\}$$

$$\mathfrak{R}_{8,r}\left[\vec{S}_{h_{r-1}},\ \vec{E}_{h_{r-1}},\vec{J}_{h_{r-1}},\ \vec{P}_{h_{r-1}},\ \vec{C}_{h_{r-1}},\ \vec{R}_{h_{r-1}},\ \vec{S}_{zv_{r-1}},\vec{E}_{zv_{r-1}},\ \vec{J}_{zv_{r-1}},\right]=\ \mathrm{L}\{\mathrm{E}_{zv_{r-1}}(\iota)\}$$
$$-\left(1-\frac{\mathrm{Kr}}{n}\right)\frac{E_{zv_0}}{s}-\frac{1}{\mathrm{B}(\wp)}\left(1-\wp+\frac{\wp}{S^{\wp}}\right)\times L\{\ \alpha\,\eta_2\sum_{i=0}^{r-1}S_{zv_{r-1-i}}(\iota)J_{h_i}(\iota)-(\gamma+\mu)E_{zv_{r-1}}(\iota)\}$$

$$\mathfrak{R}_{9,r}\left[\vec{S}_{h_{r-1}},\ \vec{E}_{h_{r-1}},\vec{J}_{h_{r-1}},\ \vec{P}_{h_{r-1}},\ \vec{C}_{h_{r-1}},\ \vec{R}_{h_{r-1}},\ \vec{S}_{zv_{r-1}},\vec{E}_{zv_{r-1}},\ \vec{J}_{zv_{r-1}},\right]=\ \mathrm{L}\{\mathrm{J}_{zv_{r-1}}(\iota)\}$$
$$-\left(1-\frac{\mathrm{Kr}}{n}\right)\frac{J_{zv_0}}{s}-\frac{1}{\mathrm{B}(\wp)}\left(1-\wp+\frac{\wp}{S^{\wp}}\right)\times L\{\ \gamma E_{h_{r-1}}(\iota)-\mu\,J_{zv_{r-1}}(\iota)\}$$

By applying inverse LT to both sides of (5), we obtain

$$\mathrm{S}_{h_r}(\iota)$$
$$=\mathrm{K_r}\mathrm{S}_{h_{r-1}}(\iota)L^{-1}\left\{\mathfrak{R}_{1,r}\left[\vec{S}_{h_{r-1}},\vec{E}_{h_{r-1}},\vec{J}_{h_{r-1}},\vec{P}_{h_{r-1}},\vec{C}_{h_{r-1}},\vec{R}_{h_{r-1}},\ \vec{S}_{zv_{r-1}},\vec{E}_{zv_{r-1}},\vec{J}_{zv_{r-1}},\right]\right\}$$

$$\mathrm{E}_{h_r}(\iota)$$
$$=\mathrm{K_r}\mathrm{E}_{h_{r-1}}(\iota)L^{-1}\left\{\mathfrak{R}_{2,r}\left[\vec{S}_{h_{r-1}},\ \vec{E}_{h_{r-1}},\vec{J}_{h_{r-1}},\ \vec{P}_{h_{r-1}},\ \vec{C}_{h_{r-1}},\ \vec{R}_{h_{r-1}},\ \vec{S}_{zv_{r-1}},\vec{E}_{zv_{r-1}},\ \vec{J}_{zv_{r-1}},\right]\right\}$$

$$\mathrm{J}_{h_r}(\iota)$$
$$=\mathrm{K_r}\mathrm{J}_{h_{r-1}}(\iota)L^{-1}\left\{\mathfrak{R}_{3,r}\left[\vec{S}_{h_{r-1}},\ \vec{E}_{h_{r-1}},\vec{J}_{h_{r-1}},\ \vec{P}_{h_{r-1}},\ \vec{C}_{h_{r-1}},\ \vec{R}_{h_{r-1}},\ \vec{S}_{zv_{r-1}},\vec{E}_{zv_{r-1}},\ \vec{J}_{zv_{r-1}},\right]\right\}$$

$$\mathrm{P}_{h_r}(\iota)$$
$$=\mathrm{K_r}\mathrm{P}_{h_{r-1}}(\iota)L^{-1}\left\{\mathfrak{R}_{4,r}\left[\vec{S}_{h_{r-1}},\ \vec{E}_{h_{r-1}},\vec{J}_{h_{r-1}},\ \vec{P}_{h_{r-1}},\ \vec{C}_{h_{r-1}},\ \vec{R}_{h_{r-1}},\ \vec{S}_{zv_{r-1}},\vec{E}_{zv_{r-1}},\ \vec{J}_{zv_{r-1}},\right]\right\}$$

$$\mathrm{C}_{h_r}(\iota)$$
$$=\mathrm{K_r}\mathrm{C}_{h_{r-1}}(\iota)L^{-1}\left\{\mathfrak{R}_{5,r}\left[\vec{S}_{h_{r-1}},\ \vec{E}_{h_{r-1}},\vec{J}_{h_{r-1}},\ \vec{P}_{h_{r-1}},\ \vec{C}_{h_{r-1}},\ \vec{R}_{h_{r-1}},\ \vec{S}_{zv_{r-1}},\vec{E}_{zv_{r-1}},\ \vec{J}_{zv_{r-1}},\right]\right\}$$

$$\mathrm{R}_{h_r}(\iota)$$
$$=\mathrm{K_r}\mathrm{R}_{h_{r-1}}(\iota)L^{-1}\left\{\mathfrak{R}_{6,r}\left[\vec{S}_{h_{r-1}},\ \vec{E}_{h_{r-1}},\vec{J}_{h_{r-1}},\ \vec{P}_{h_{r-1}},\ \vec{C}_{h_{r-1}},\ \vec{R}_{h_{r-1}},\ \vec{S}_{zv_{r-1}},\vec{E}_{zv_{r-1}},\ \vec{J}_{zv_{r-1}},\right]\right\}$$

$$S_{zv_r}(\iota) = K_r S_{zv_{r-1}}(\iota) L^{-1}\left\{\Re_{7,r}\left[\vec{S}_{h_{r-1}}, \vec{E}_{h_{r-1}}, \vec{J}_{h_{r-1}}, \vec{P}_{h_{r-1}}, \vec{C}_{h_{r-1}}, \vec{R}_{h_{r-1}}, \vec{S}_{zv_{r-1}}, \vec{E}_{zv_{r-1}}, \vec{J}_{zv_{r-1}},\right]\right\}$$

$$E_{zv_r}(\iota) = K_r E_{zv_{r-1}}(\iota) L^{-1}\left\{\Re_{8,r}\left[\vec{S}_{h_{r-1}}, \vec{E}_{h_{r-1}}, \vec{J}_{h_{r-1}}, \vec{P}_{h_{r-1}}, \vec{C}_{h_{r-1}}, \vec{R}_{h_{r-1}}, \vec{S}_{zv_{r-1}}, \vec{E}_{zv_{r-1}}, \vec{J}_{zv_{r-1}},\right]\right\}$$

$$J_{zv_r}(\iota) = K_r J_{zv_{r-1}}(\iota) L^{-1}\left\{\Re_{9,r}\left[\vec{S}_{h_{r-1}}, \vec{E}_{h_{r-1}}, \vec{J}_{h_{r-1}}, \vec{P}_{h_{r-1}}, \vec{C}_{h_{r-1}}, \vec{R}_{h_{r-1}}, \vec{S}_{zv_{r-1}}, \vec{E}_{zv_{r-1}}, \vec{J}_{zv_{r-1}},\right]\right\} \quad (6)$$

On solving the above system, we get

$S_{h_0}(\iota) = 500$

$E_{h_0}(\iota) = 110$

$J_{h_0}(\iota) = 75$

$P_{h_0}(\iota) = 10$

$C_{h_0}(\iota) = 5$

$R_{h_0}(\iota) = 10$

$S_{zv_0}(\iota) = 500$

$E_{zv_0}(\iota) = 95$

$J_{zv_0}(\iota) = 70$

$$S_{h_1} = \frac{-5.86500\,h}{B(\wp)}\left\{1 - \wp + \frac{\wp\, t^{\wp}}{\Gamma(\wp+1)}\right\}$$

$$E_{h_1} = \frac{17.40060\,h}{B(\wp)}\left\{1 - \wp + \frac{\wp\, t^{\wp}}{\Gamma(\wp+1)}\right\}$$

$$J_{h_1} = \frac{-19.25400\,h}{B(\wp)}\left\{1 - \wp + \frac{\wp\, t^{\wp}}{\Gamma(\wp+1)}\right\}$$

$$P_{h_1} = \frac{-24.71460\,h}{B(\wp)}\left\{1 - \wp + \frac{\wp\, t^{\wp}}{\Gamma(\wp+1)}\right\}$$

$$C_{h_1} = \frac{-1.64980\,h}{B(\wp)}\left\{1 - \wp + \frac{\wp\, t^{\wp}}{\Gamma(\wp+1)}\right\}$$

$$R_{h_1} = \frac{-15.88960\,h}{B(\wp)}\left\{1 - \wp + \frac{\wp\, t^{\wp}}{\Gamma(\wp+1)}\right\}$$

$$S_{zv_1} = \frac{75977.8000\,h}{B(\wp)}\left\{1 - \wp + \frac{\wp\, t^{\wp}}{\Gamma(\wp+1)}\right\}$$

$$E_{zv_1} = \frac{-1034.1635\ h}{B(\wp)}\left\{1-\wp+\frac{\wp\, t^{\wp}}{\mathbb{\Gamma}(\wp+1)}\right\}$$

$$J_{h_1} = \frac{-6.6625\ h}{B(\wp)}\left\{1-\wp+\frac{\wp\, t^{\wp}}{\mathbb{\Gamma}(\wp+1)}\right\}$$

$$S_{h_2} = \frac{-5.86500\ h\ (n\ +\ h)}{B(\wp)}\left\{1-\wp+\frac{\wp\, t^{\wp}}{\mathbb{\Gamma}(\wp+1)}\right\} - \frac{9.960960450\mathfrak{h}^2}{[\mathcal{B}(\wp)]^2}\left(1-2\wp+\wp^2+\frac{2\wp(1-\wp)t^{\wp}}{\Gamma(\wp+1)}+\frac{\wp^2 t^{2\wp}}{\Gamma(2\wp+1)}\right)$$

$$E_{h_2} = \frac{17.40060\ h\ (n\ +\ h)}{B(\wp)}\left\{1-\wp+\frac{\wp\, t^{\wp}}{\mathbb{\Gamma}(\wp+1)}\right\} + \frac{1.347048000\mathfrak{h}^2}{[\mathcal{B}(\wp)]^2}\left(1-2\wp+\wp^2+\frac{2\wp(1-\wp)t^{\wp}}{\Gamma(\wp+1)}+\frac{\wp^2 t^{2\wp}}{\Gamma(2\wp+1)}\right)$$

$$J_{h_2} = \frac{-19.25400\ h\ (n\ +\ h)}{B(\wp)}\left\{1-\wp+\frac{\wp\, t^{\wp}}{\mathbb{\Gamma}(\wp+1)}\right\} - \frac{8.557562940\mathfrak{h}^2}{[\mathcal{B}(\wp)]^2}\left(1-2\wp+\wp^2+\frac{2\wp(1-\wp)t^{\wp}}{\Gamma(\wp+1)}+\frac{\wp^2 t^{2\wp}}{\Gamma(2\wp+1)}\right)$$

$$P_{h_2} = \frac{-24.71460h\ (n\ +\ h)}{B(\wp)}\left\{1-\wp+\frac{\wp\, t^{\wp}}{\mathbb{\Gamma}(\wp+1)}\right\} - \frac{26.76811163\mathfrak{h}^2}{[\mathcal{B}(\wp)]^2}\left(1-2\wp+\wp^2+\frac{2\wp(1-\wp)t^{\wp}}{\Gamma(\wp+1)}+\frac{\wp^2 t^{2\wp}}{\Gamma(2\wp+1)}\right)$$

$$C_{h_2} = \frac{-1.64980\ h\ (n\ +\ h)}{B(\wp)}\left\{1-\wp+\frac{\wp\, t^{\wp}}{\mathbb{\Gamma}(\wp+1)}\right\} - \frac{4.399068008\ \mathfrak{h}^2}{[\mathcal{B}(\wp)]^2}\left(1-2\wp+\wp^2+\frac{2\wp(1-\wp)t^{\wp}}{\Gamma(\wp+1)}+\frac{\wp^2 t^{2\wp}}{\Gamma(2\wp+1)}\right)$$

$$R_{h_2} = \frac{-15.88960\ h\ (n\ +\ h)}{B(\wp)}\left\{1-\wp+\frac{\wp\, t^{\wp}}{\mathbb{\Gamma}(\wp+1)}\right\} + \frac{15.16390081\mathfrak{h}^2}{[\mathcal{B}(\wp)]^2}\left(1-2\wp+\wp^2+\frac{2\wp(1-\wp)t^{\wp}}{\Gamma(\wp+1)}+\frac{\wp^2 t^{2\wp}}{\Gamma(2\wp+1)}\right)$$

$$S_{zv_2} = \frac{1.520556000\ *10^5\ h\ (n\ +\ h)}{B(\wp)}\left\{1-\wp+\frac{\wp\, t^{\wp}}{\mathbb{\Gamma}(\wp+1)}\right\} + \frac{2.313538529\ *10^7\mathfrak{h}^2}{[\mathcal{B}(\wp)]^2}\left(1-2\wp+\wp^2+\frac{2\wp(1-\wp)t^{\wp}}{\Gamma(\wp+1)}+\frac{\wp^2 t^{2\wp}}{\Gamma(2\wp+1)}\right)$$

$$E_{zv_2} = \frac{-2084.1635\ h\ (n\ +\ h)}{B(\wp)}\left\{1-\wp+\frac{\wp\ t^{\wp}}{\mathbb{\Gamma}(\wp+1)}\right\} - \frac{3.189384301\ *10^5\ \mathfrak{h}^2}{[\mathcal{B}(\wp)]^2}\left(1-2\wp+\wp^2+\frac{2\wp(1-\wp)t^{\wp}}{\Gamma(\wp+1)}+\frac{\wp^2 t^{2\wp}}{\Gamma(2\wp+1)}\right)$$

$$J_{zv_2} = \frac{-6.6625\ h\ (n\ +\ h)}{B(\wp)}\left\{1-\wp+\frac{\wp\ t^{\wp}}{\mathbb{\Gamma}(\wp+1)}\right\} + \frac{231.1801298\mathfrak{h}^2}{[\mathcal{B}(\wp)]^2}\left(1-2\wp+\wp^2+\frac{2\wp(1-\wp)t^{\wp}}{\Gamma(\wp+1)}+\frac{\wp^2 t^{2\wp}}{\Gamma(2\wp+1)}\right) \quad (7)$$

and so forth, the values provided can be obtained by simplifying the system of equations mentioned above. We acquire the series as given by the q - HATM solutions

$$\begin{aligned}
S_h(\iota) &= S_{h0}(\iota)+\sum_{r=1}^{\infty} S_{hm}(\iota)\left(\frac{1}{\mathfrak{m}}\right)^r\\
E_h(\iota) &= E_{h0}(\iota)+\sum_{r=1}^{\infty} E_{hm}(\iota)\left(\frac{1}{\mathfrak{m}}\right)^r\\
J_h(\iota) &= J_{h0}(\iota)+\sum_{r=1}^{\infty} J_{hm}(\iota)\left(\frac{1}{\mathfrak{m}}\right)^r\\
P_h(\iota) &= P_{h0}(\iota)+\sum_{r=1}^{\infty} P_{hm}(\iota)\left(\frac{1}{\mathfrak{m}}\right)^r\\
C_h(\iota) &= C_{h0}(\iota)+\sum_{r=1}^{\infty} C_{hm}(\iota)\left(\frac{1}{\mathfrak{m}}\right)^r\\
R_h(\iota) &= R_{h0}(\iota)+\sum_{r=1}^{\infty} R_{hm}(\iota)\left(\frac{1}{\mathfrak{m}}\right)^r\\
S_{zv}(\iota) &= S_{zv0}(\iota)+\sum_{r=1}^{\infty} S_{hm}(\iota)\left(\frac{1}{\mathfrak{m}}\right)^r\\
E_{zv}(\iota) &= E_{zv0}(\iota)+\sum_{r=1}^{\infty} E_{hm}(\iota)\left(\frac{1}{\mathfrak{m}}\right)^r\\
J_{zv}(\iota) &= J_{zv0}(\iota)+\sum_{r=1}^{\infty} J_{hm}(\iota)\left(\frac{1}{\mathfrak{m}}\right)^r
\end{aligned} \quad (8)$$

7. Results and discussion

This section presents and discusses the analytical and numerical findings of the proposed Zika virus transmission model. The discussion is organized into two main parts. First, the stability properties of the equilibrium points are analyzed using the Jacobian matrix and Routh–Hurwitz criteria. Second, approximate analytical solutions obtained via the q-Homotopy Analysis Transform Method (q-HATM) are examined to illustrate the dynamic behaviour of the system. The stability behaviour of the proposed model is governed by the nature of its equilibrium points. In particular, the disease-free and endemic equilibria determine whether the Zika virus dies out or persists in the population. The disease-free equilibrium corresponds to the absence of infection in both human and mosquito populations. To investigate its stability, the Jacobian matrix of the system is derived and evaluated at the disease-free equilibrium. The resulting Jacobian matrix exhibits a block structure, separating infected and uninfected compartments.

The characteristic equation obtained from the Jacobian matrix yields a polynomial whose coefficients depend on the epidemiological parameters. By applying the Routh–Hurwitz stability criteria, it is shown that all the roots of the characteristic equation have negative real parts whenever the basic reproduction number satisfies $R_0 < 1$. This result implies that the disease-free equilibrium is locally asymptotically stable, and small perturbations around this equilibrium decay over time. Epidemiologically, this indicates that the Zika virus cannot invade the population when transmission potential is below the critical threshold. However, when the Routh–Hurwitz conditions are violated, leading to at least one eigenvalue with a positive real part. In this case, the disease-free equilibrium becomes unstable, allowing the disease to spread. The Jacobian matrix evaluated at the endemic equilibrium produces a characteristic polynomial with higher degree nonlinear terms. Using the Routh–Hurwitz criteria, sufficient conditions are derived to ensure that all eigenvalues have negative real parts. The analysis confirms that the endemic equilibrium is locally asymptotically stable. After establishing the stability properties of the model, we employ simulation of the model without any interventions, representing the uncontrolled scenario, shows a rapid increase in infected humans and vectors, with infection levels reaching high peaks over time. This indicates that, in the absence of prevention, treatment, or vector management measures, the disease can persist and spread widely within the population. Incorporating optimal control strategies significantly reduces the number of infected individuals and vectors, flattens the infection peaks, and shortens the duration of the outbreak. Comparing the uncontrolled and controlled scenarios highlights the effectiveness of time-dependent interventions and emphasizes the importance of coordinated strategies for disease mitigation. The q-Homotopy Analysis Transform Method (q-HATM) is employed to obtain approximate analytical solutions of the nonlinear system. The q-HATM provides a flexible framework by introducing an auxiliary convergence-control parameter, which ensures rapid convergence of the solution series. Unlike traditional numerical schemes, the method yields explicit series solutions that capture the nonlinear interaction between human and mosquito populations. The method is applied to each compartment of the model, and the approximate solutions are constructed iteratively. The convergence of the solution series is ensured by selecting appropriate values of the auxiliary parameter. Together, these results offer a comprehensive understanding of Zika virus transmission dynamics and provide valuable guidance for disease control policies.

ι	$\wp = 0.6$	$\wp = 0.7$	$\wp = 0.8$	$\wp = 0.9$	$\wp = 1$
0	523.9396097	517.6558784	511.5713664	505.6860736	500
50	1327.994808	2193.762117	4018.364906	7838.449938	15744.43256
100	2020.818353	4193.582690	9625.494829	9625.494829	55891.26625
150	2720.277483	6480.764838	16863.14309	45177.31048	1.2094050×10^5

Table 1. The susceptible class table for S_h (ι) for different $\wp$ values

ι	$\wp = 0.6$	$\wp = 0.7$	$\wp = 0.8$	$\wp = 0.9$	$\wp = 1$
0	109.1760077	104.3415943	99.53412192	94.75359048	90
50	497.6934575	805.6584225	1356.344635	2347.153860	4143.870000
100	735.6745411	1372.522332	2694.581041	5500.397225	11565.36000
150	947.0640032	1934.892042	4195.423757	9524.613864	22354.47000

Table 2. The exposed class table for E_h (ι) for different $\wp$ values

ι	$\wp = 0.6$	$\wp = 0.7$	$\wp = 0.8$	$\wp = 0.9$	$\wp = 1$
0	84.07081007	81.54638066	79.19310252	77.01097563	75
50	573.0451388	1179.156016	2527.469376	5467.313161	11734.65368
100	1064.186505	2683.422868	6926.300514	17775.04737	44788.21470
150	1580.855417	4465.835372	12767.68296	36010.64010	99235.68308

Table 3. The infected class table for J_h (ι) for different $\wp$ values

ι	$\wp = 0.6$	$\wp = 0.7$	$\wp = 0.8$	$\wp = 0.9$	$\wp = 1$
0	24.16873786	19.82351005	16.01364446	12.73914112	10
50	1304.335046	3030.133024	6976.787801	15750.01299	34705.86954
100	2712.035218	7471.311065	20219.47899	53275.55022	1.363220182×10^5
150	4224.084479	12821.16930	38026.07553	1.093931946×10^5	3.048584458×10^5

Table 4. The pregnant class table for P_h (ι) for different $\wp$ values

ι	$\wp = 0.6$	$\wp = 0.7$	$\wp = 0.8$	$\wp = 0.9$	$\wp = 1$
0	6.363770881	5.890856121	5.505922720	5.208970680	5
50	199.8116716	471.8753670	1102.071465	2515.159651	5586.325010

100	422.4195522	1183.796366	3243.269751	8616.011343	22165.32004
150	663.8399780	2047.673900	6138.003761	17775.66479	49741.98509

Table 5. The infant class table for C_h (ι) for different $\wp$ values

ι	$\wp = 0.6$	$\wp = 0.7$	$\wp = 0.8$	$\wp = 0.9$	$\wp = 1$
0	18.93479552	16.21754248	13.82265888	11.75014472	10
50	796.8647656	1840.884650	4225.056891	9519.863988	20952.57001
100	1648.163075	4522.644960	12213.83640	32143.55404	82191.32005
150	2561.600244	7750.472492	22949.31662	65961.10763	1.837262501×10^{5}

Table 6. The recovered class table for R_h (ι) for different $\wp$ values

ι	$\wp = 0.6$	$\wp = 0.7$	$\wp = 0.8$	$\wp = 0.9$	$\wp = 1$
0	3.641379406×10^{6}	2.037097996×10^{6}	8.955242916×10^{5}	2.166582929×10^{5}	500
50	9.590245011×10^{8}	2.347556879×10^{9}	5.594514567×10^{9}	1.292109872×10^{10}	2.891163433×10^{10}
100	2.097785037×10^{9}	6.025984179×10^{9}	1.672691082×10^{10}	4.476450287×10^{10}	1.156617313×10^{11}
150	3.341574228×10^{9}	1.051318047×10^{10}	3.183509605×10^{10}	9.270698552×10^{10}	2.602502917×10^{11}

Table 7. The susceptible vector class table for S_{zv} (ι) for different $\wp$ values

ι	$\wp = 0.6$	$\wp = 0.7$	$\wp = 0.8$	$\wp = 0.9$	$\wp = 1$
0	51958.81422	29424.70776	13269.36990	3492.800651	95
50	1.325196593×10^{7}	3.241393316×10^{7}	7.720752734×10^{7}	1.782596527×10^{8}	3.987773408×10^{8}
100	2.896575635×10^{7}	8.315486725×10^{7}	2.307366845×10^{8}	6.173590921×10^{8}	1.594900661×10^{9}
150	4.612456165×10^{7}	1.450407342×10^{8}	4.390689673×10^{8}	1.278390407×10^{9}	3.588370059×10^{9}

Table 8. The exposed vector class table for E_{zv} (ι) for different $\wp$ values

ι	$\wp = 0.6$	$\wp = 0.7$	$\wp = 0.8$	$\wp = 0.9$	$\wp = 1$
0	109.6538208	92.80496168	80.57970519	72.97805130	70
50	9713.753559	23627.84162	56135.43941	1.294436261×10^{5}	2.893782872×10^{5}
100	21122.43203	60445.35219	1.674948829×10^{5}	4.478627371×10^{5}	1.156636899×10^{6}
150	33574.96459	1.053355784×10^{5}	3.185704761×10^{5}	9.271402899×10^{5}	2.601845835×10^{6}

Table 9. The infected vector class table for J_{zv} (ι) for different $\wp$ values

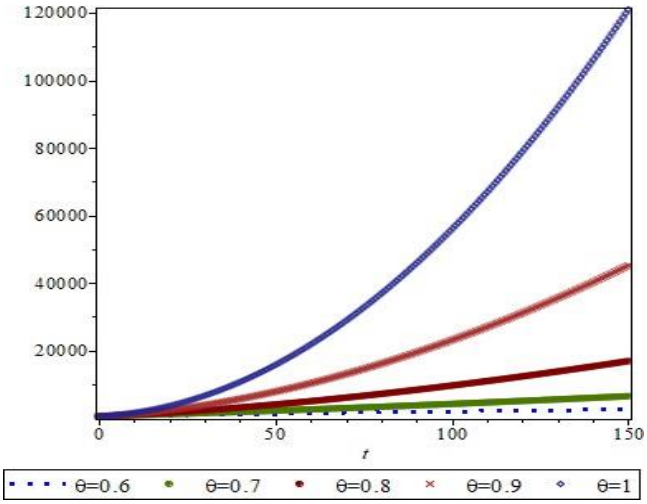

FIGURE 1. Plot of q − HATM solution for $S_h(\iota)$ with respect to ι at $h = -1, m = 1$ for varying θ.

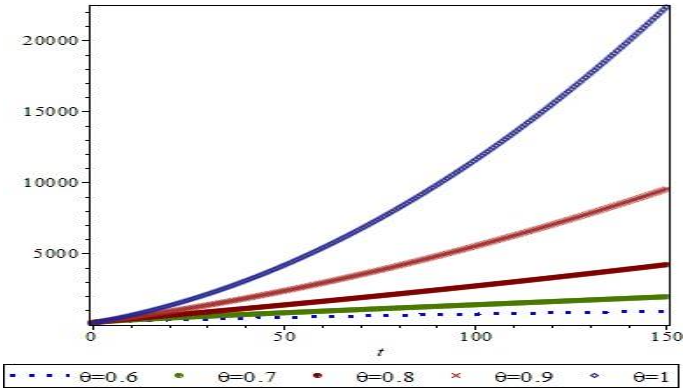

FIGURE 2. Plot of q − HATM solution for $E_h(\iota)$ with respect to ι at $h = -1; m = 1$, for varying θ.

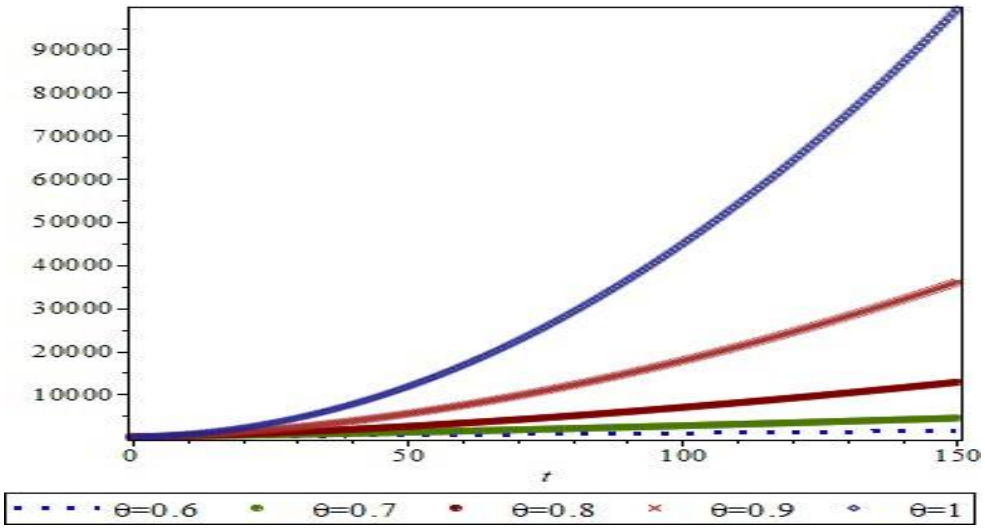

FIGURE 3. Plot of q − HATM solution for $J_h(\iota)$ with respect to ι at $h = -1, m = 1$, for varying θ.

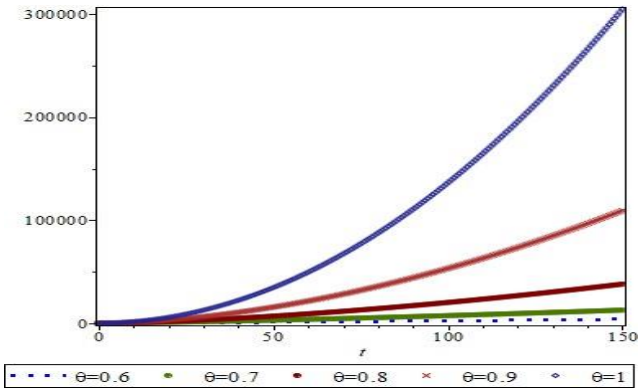

FIGURE 4. Plot of q − HATM solution for $P_h(\iota)$ with respect to ι at $h = -1, ; m = 1$, for varying θ.

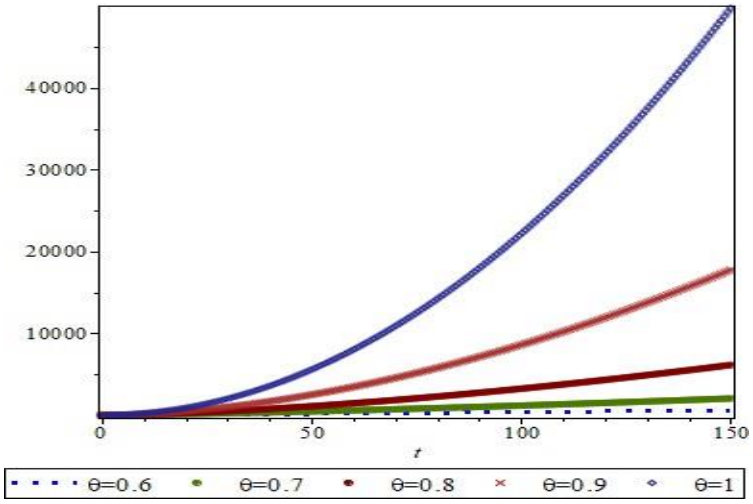

FIGURE 5. Plot of q − HATM solution for $C_h(\iota)$ with respect to ι at $h = -1, ; m = 1$, for varying θ.

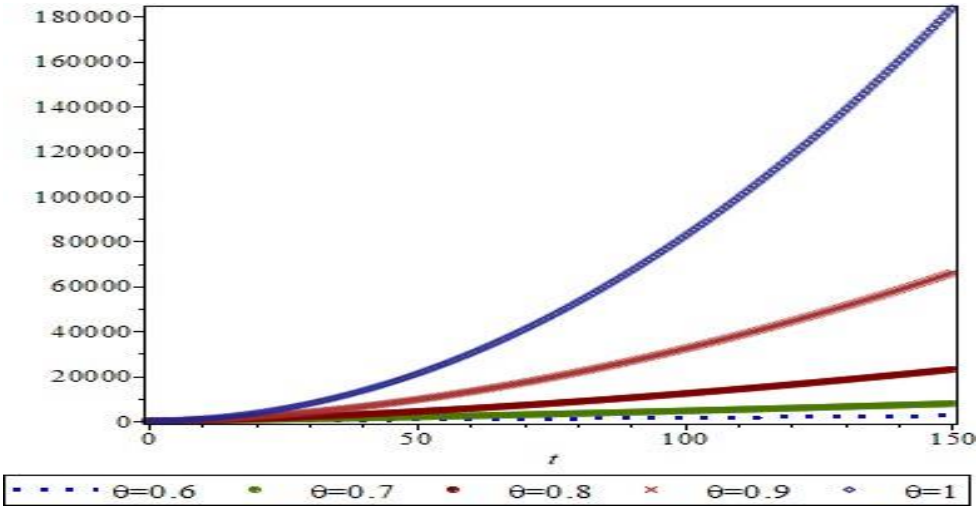

FIGURE 6. Plot of q − HATM solution for $R_h(\iota)$ with respect to ι at $h = -1, ; m = 1$, for varying θ.

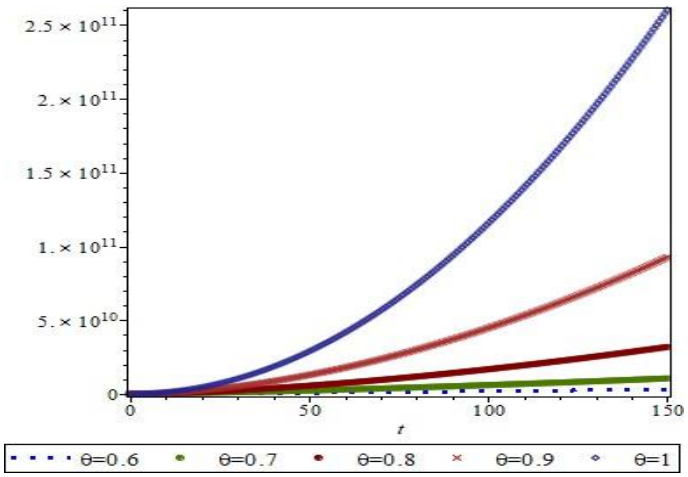

FIGURE 7. Plot of q − HATM solution for $S_{zv}(\iota)$ with respect to ι at $h = -1, ; m = 1$, for varying θ.

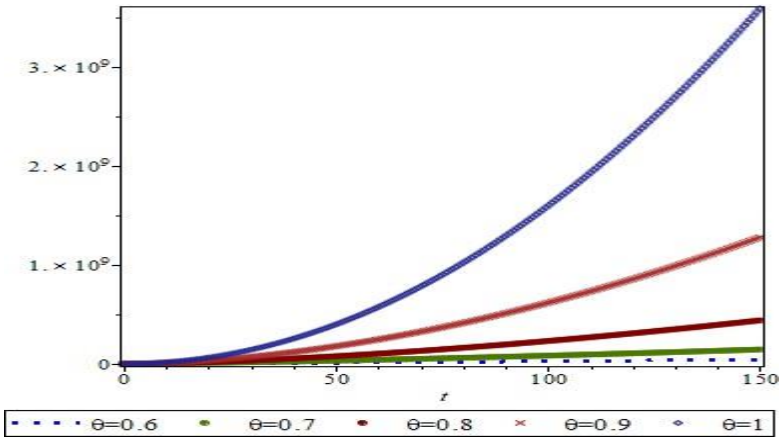

FIGURE 8. Plot of q − HATM solution for $E_{zv}(\iota)$ with respect to ι at $h = -1, ; m = 1$, for varying θ.

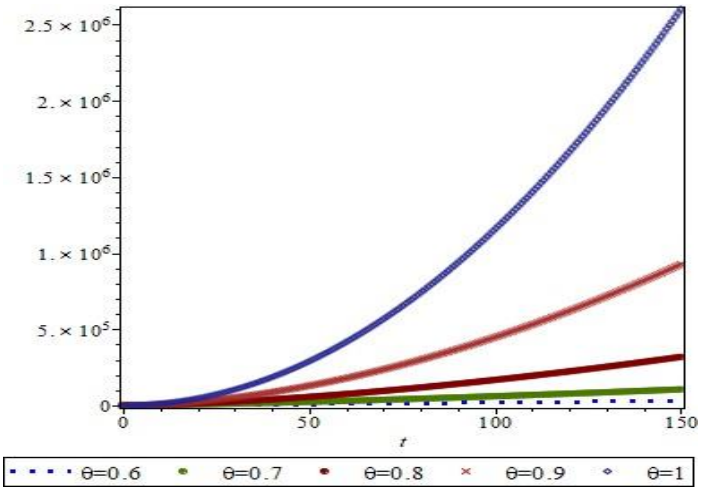

FIGURE 9. Plot of q − HATM solution for $J_{zv}(\iota)$ with respect to ι at h= −1, ; m = 1, for varying θ.

8. Conclusion

In this work, a comprehensive mathematical model has been developed to investigate the transmission dynamics of the Zika virus involving both human and mosquito populations. The model incorporates multiple epidemiologically relevant compartments, including exposed, infected, recovered, pregnant women, and infected infants, allowing a more realistic representation of disease progression and public health impact. The qualitative analysis of the model reveals the existence of biologically meaningful equilibrium points. Using the Jacobian matrix and the Routh–Hurwitz stability criteria, it is shown that the disease-free equilibrium is locally asymptotically stable when the basic reproduction number is less than unity. This result confirms that Zika virus transmission can be effectively eliminated if control measures reduce the transmission potential below the critical threshold. Conversely, when the reproduction number exceeds one, the disease-free equilibrium becomes unstable and a unique endemic equilibrium emerges, which is proven to be locally asymptotically stable, indicating persistent circulation of the virus in the population. Optimal control analysis indicates that coordinated prevention, treatment, and vector control strategies are effective in minimizing infections and associated costs in the human-vector system. To complement the analytical findings, the q-Homotopy Analysis Transform Method (q-HATM) is employed to obtain approximate analytical solutions of the nonlinear system. The q-HATM solutions demonstrate excellent convergence and provide clear insight into the temporal evolution of all compartments. The numerical results support the theoretical stability analysis, showing convergence toward the disease-free equilibrium when transmission is weak and stabilization around the endemic equilibrium when transmission is sustained. The results highlight the critical role of mosquito dynamics in driving Zika virus transmission and emphasize the importance of vector control strategies. Parameters associated with mosquito mortality, transmission rates, and treatment significantly influence disease prevalence. In particular, the inclusion of pregnancy-related compartments underscores the severe consequences of Zika virus infection and the necessity of targeted intervention strategies for vulnerable populations. Overall, the proposed model and analytical framework offer valuable insights into the transmission mechanisms of Zika virus and provide a robust mathematical foundation for evaluating control and prevention strategies. Future work may extend the model to include spatial effects, seasonal variability, stochastic influences, or optimal control measures to further enhance its applicability in real-world epidemiological settings.

Refrences

[1] M. Abdullah, A. Ahmad, N. Raza, M. Farman and M. O. Ahmad, Approximate solution and analysis of smoking epidemic model with Caputo fractional derivatives, Int. J. Appl. Comput. Math., **4** (5) (2018), 1—16, doi:10.1007/s40819-018-0543-5.

[2] K. D. Ahmed, M.O. Ibrahim and A. Gambo, Deterministic model of Zika virus with carrier mother and reservoirs. FUDMA J. Sci., **8** (2024), 316—331, doi: 10.33003/fjs-2024-0803-2401.

[3] E. Alzahrani and A. Zeb, Stability analysis and prevention strategies of tobacco smoking model, Bound. Value Probl., **3** (2020), 1–13, doi: 10.1186/s13661-019-01315-1.

[4] P. Andayani, L. R. Sari, A. Suryanto and I. Darti, Numerical study for Zika virus

transmission with beddington-deangelis incidence rate, Far East J. Math. Sci., **111** (1) (2019), 145–157, doi:10.17654/MS111010145.

[5] A. Atangana and J. F. Gómez-Aguilar, A new derivative with normal distribution kernel, Theo. Meth. Appl. Phys. A, **476** (2017), 1—14, doi:10.1016/j.physa.2017.02.016.

[6] A. Atangana and J. F. Gómez-Aguilar, Hyperchaotic behaviour obtained via a nonlocal operator with exponential decay and Mittag-Leffler laws, Chaos Solitons Fractals, **102** (2017), 285–294, doi:10.1016/j.chaos.2017.03.022.

[7] C. Bhunu and S. Mushayabasa, Modelling the transmission dynamics of pox like infections, Int. J Appl. Math., **41** (2) (2011), 1–9.

[8] K.S. Chiu and F. Córdova-Lepe, Existence and global exponential stability of equilibrium for an epidemic model with piecewise constant argument, Axioms, **14** (2025), 514, doi:10.3390/axioms14070514.

[9] G. Chowell, N. W. Hengartner, C. Castillo-Chavez, P. W. Fenimore and J. M. Hyman, The basic reproduc- tive number of Ebola and the effects of public health measures: the cases of Congo and Uganda, J. Theor. Biol., **229** (2004), 119—126. doi:10.1016/j.jtbi.2004.03.006.

[10] O. Diekmann, J. A. P. Heesterbeek and J. A. J. Metz, On the definition and the computation of the basic reproduction ratio, J. Math. Biol., **28** (1990), 365—382, doi :10.1007/BF00178324.

[11] A. K. Dotia, M. O. Ibrahim, A. Gambo, A. B. Musa and A. O. Lawani, Deterministic model of Zika virus with carrier mother and reservoirs: A mathematical analysis approach, FUDMA J. Sci., **8** (3) (2024), 316–331, doi:10.33003/fjs-2024-0803-2401.

[12] Y. Du, Y. Chen and Q. Zhang, Averaging principle and optimal control for a two-time-scale stochastic reaction-diffusion HIV model, Adv. Contin. Discrete Models, **177** (2025), 1–24. doi:10.1186/s13662-025- 04036-1.

[13] E. C. Duru, G. C. E. Mbah, M. C. Anyanwu and N. N. Topman, Modelling the co-infection of malaria and Zika virus disease, J. Nig.Soc. Phys. Sci., **6** (2) (2024), 1938, doi:1046481/jnsps.2024.1938.

[14] E. C. Duru, G. C. E. Mbah and A. Uzoma, Numerical Simulations and Solutions of a Mathematical Model for Zika Virus Disease, Appl. Model. Simul., **9** (2) (2025), 139–153.

[15] M. Farman, N. Ahmad and M. Raza, q-HATM solution of nonlinear biological models, Alex. Eng. J., **59** (2020), 315—324, doi:10.1016/j.aej.2019.12.015.

[16] D. Gao, Y. Lou, D. He, T. C. Porco, Y.Kuang and G. Chowell, Prevention and control of Zika virus transmission, Sci. Rep., **6** (2016), 28070, doi:10.1038/srep28070.

[17] H. F. Huo, R. Chen and X. Y. Wang, Modelling and stability of HIV/AIDS epidemic

model with treatment, Appl. Math. Model., **40** (13) (2016), 6550–6559, doi:10.1016/j.apm.2016.01.054.

[18] M. A. Ibrahim and A. Denes, A mathematical model for Zika virus infection and microcephaly risk con- sidering sexual and vertical transmission, Axioms, **12** (2023), 263, doi:10.3390/axioms12030263

[19] A. Kouidere, A. E. Bhih, I. Minifi, O. Balatif and K. Adnaoui, Optimal control problem for mathemat- ical modelling of Zika virus transmission using fractional order derivatives, Front. Appl. Math. Stat., **10** (1376507) (2024), doi:10.3389/fams.2024.1376507.

[20] Z.N. Li, Y.L. Tang and Z. Wang, Optimal control of a COVID-19 dynamics based on SEIQR model, Adv. Contin. Discrete Models, 50 (2025), 1–21, doi:10.1186/s13662.025.03869.0.

[21] K. M. Owolabi and A. Atangana, Mathematical analysis and computational experiments for an epidemic system with nonlocal and nonsingular derivative, Chaos Solitons and Fractals, **126** (2019), 41–49, doi:10.1016/j.chaos.2019.06.001

[22] V. Padmavathi, N. Magesh , K. Alagesan , M. I. Khan, S. Elattar, M. Alwetaishi, and A. M. Galal, Numerical modeling and symmetry analysis of a pine wilt disease model using the Mittag leffler kernel, Symmetry, **14** (2022), 1—15, doi:10.3390/sym14051067.

[23] V. Padmavathi, A. Prakash, K. Alagesan and N. Magesh, Analysis and numerical simulation of novel coronavirus (COVID-19) model with Mittag-Leffler Kernel. Math. Method Appl. Sci., **44** (2) (2021), 1863— 1877, doi:10.1002/mma.6886.

[24] S. Pathak, A. Maiti, G. Samanta and Rich dynamics of an SIR epidemic model, Nonlinear Anal. Model. Control, **15** (1) (2010), 71—81, doi:10.15388/NA.2010.15.1.14365.

[25] A. Prakash and H. Kaur, Numerical solution for fractional model of Fokker-Planck equation by using q-HATM, Chaos Solitons Fractals **105** (2017), 99—110, doi:10.1016/j.chaos.2017.10.003.

[26] A. Prakash and H. Kaur, Analysis and numerical simulation of fractional order Chan-Allen model with Atangana-Baleanu derivatives, Chaos Solitons Fractals, **124** (2019), 134–142, doi:10.1016/j.chaos.2019.05.005.

[27] A. Prakash, M. Goyal, H. M. Baskonus and S. Gupta, A reliable hybrid numerical method for a time dependent vibration model of arbitrary order, AIMS Math., **5** (2) (2020), 979—1000, doi:10.3934/math.2020068.

[28] J. Singh, D. Kumar and D. Baleanu, New aspects of fractional Biswas-Milovic model with Mittag-Leffler law, Math. Model. Nat. Phenom., **14** (3) (2019), 1–23, doi:10.1051/mmnp/2018068.

[29] J. Sujatha and N. Magesh, An analytical approach to solve Nipah virus infection model, Commun. Appl. Nonlinear Anal. 32 (9s), (2025), doi:10.52783/cana.v32.4452.

[30] J. Sujatha, N. Magesh and G. Tamil preethi, An analytical approach for a deterministic epidemiological model- Monkeypox clinical disease, Commun. Math. Appl., 16 (2), (2025), 615–629, doi:10.26713/cma.vi6i2.3052.

[31] G. Tamil Preethi and N. Magesh, An application of differential transform method to Solve an epidemic Model — Ebola Virus disease outbreaks, Commun. Math. Appl., 14 (4), (2023), 1301–1310, doi:10.26713/cma.v14i4.2512.

[32] G. Tamil Preethi, N. Magesh and N. B. Gatti , An application of conformable fractional differential transform method for smoking epidemic model, Springer Proc. Math. Comput., 415 (2023), 339–411, doi:10.1016/j.matcom.2022.02.021.

[33] P. Veeresha, D. G. Prakasha and H. M. Baskonus, Solving smoking epidemic model of fractional order using a modefied homotopy analysis transform method, Math. Sci., **13** (2) (2019), 115—128, doi:10.1007/s40096-019-0284-6.

[34] P. Veeresha, D. G. Prakasha, N. Magesh, A. John Christopher and D. U. Sarwe, Solution for fractional potential KdV and Benjamin equations using the novel technique, J. Ocean Eng Sci., **6** (2021), 265–275, doi:10.1016/j.joes.2021.01.003.

[35] X. Wang and Y. Cai, Optimal control of an influenza model incorporating pharmacological and non- pharmacological interventions, Adv. Contin. Discrete Models, **17** (2025), 1–19, doi:10.1186/s13662-025-03867-2.

[36] World Health Organization (WHO), Zika virus fact sheet, WHO Press, Geneva, 2024

[37] H.M. Yang, M.L.G. Macoris and K.C. Galvani, Assessing the effects of control measures on Zika virus dynamics, Math. Biosci, **304** (2018), 35—44, doi:10.1016/j.mbs.2018.06.004.

[38] H. M. Youssef, N. Alahamdi, M. A. Ezzat, A. A. Elbary and A. M. Shawky, A proposed modified SEIQR epidemic model to analyze the COVID-19 spreading in Saudi Arabia, Alexandria Eng journal, **61** (2022), 2456–2470, doi:10.1016/j.aej.2021.06.095

[39] Q. Zhang, K. Sun and M. Chinazzi, Spread of Zika virus through sexual transmission, Proc. Natl. Acad. Sci. USA, **114** (2017), E4334—E4343, doi:10.1073/pnas.1621412114.

[40] A. Zeb and E. Alzahrani, Optimal control strategies for Zika virus model. Chaos Solitons Fractals, **130** (2020), 109456.